

AMCoR

Asahikawa Medical University Repository <http://amcor.asahikawa-med.ac.jp/>

Biochimica et Biophysica Acta (BBA) – General Subjects (2014.12)
1840 (12) :3345–3356.

Scavenger receptor CL-P1 mainly utilizes a collagen-like domain to uptake microbes and modified LDL

Kenichiro Mori, Katsuki Ohtani, SeongJae Jang, YounUck Kim, Insu Hwang, Nitai Roy, Yasuyuki Matsuda, Yasuhiko Suzuki, Nobutaka Wakamiya,

Scavenger receptor CL-P1 mainly utilizes a collagen-like domain to uptake microbes
and modified LDL

Kenichiro Mori^{a, 1}, Katsuki Ohtani^{a, 1}, SeongJae Jang^a, YounUck Kim^{a, b}, Insu Hwang^a, Nitai Roy^a
Yasuyuki Matsuda^a, Yasuhiko Suzuki^c, Nobutaka Wakamiya^{a,*}

^aDepartment of Microbiology & Immunochemistry, Asahikawa Medical University, Asahikawa
078-8510, Japan

^bDepartment of Biomedical Sciences, University of Sun Moon, Asan city 336-708, Korea

^cDepartment of Bioresources, Research Center for Zoonosis Control, Hokkaido University, Sapporo
001-0020, Japan

Running head: CL-P1, collectin as well as scavenger receptor, has multi-sites for ligand binding

¹The first two authors contributed equally to this work.

*to whom correspondence should be addressed: Dept. of Microbiology and Immunochemistry,
Asahikawa Medical University, 2-1-1 Midorigaoka-Higashi, Asahikawa 078-8510 Japan.

[Tel:81-166-68-2393](tel:81-166-68-2393); Fax:81-166-68-2399; E-mail address: wakamiya@asahikawa-med.ac.jp

Keywords: Collectin, Scavenger Receptor, Endocytosis, Phagocytosis, Collagen, OxLDL

ABSTRACT

Background: Collectins are considered to play a role in host defense via complement activation and opsonization, and are composed of a collagen-like domain and a carbohydrate recognition domain (CRD). Collectin placenta 1 (CL-P1) showed scavenger receptor activity as functions in vitro, and has three candidate domains: a coiled-coil domain, a collagen-like domain and CRD.

Methods: We constructed seven types of CL-P1 deletion mutants to determine the site of each ligand binding domain, and observed whether the specific binding to sugar ligand, microbes, or oxidized LDL decreases or not in cells with CL-P1 deletion mutants and CL-P1 containing mutations of amino acid, respectively.

Results: CL-P1 mainly interacted with ligands of microbes through the collagen-like domain and it binds a sugar ligand through the CRD. Additionally it could bind oxidized low density lipoprotein (OxLDL) due to the coiled-coil domain as well as the collagen-like domain. This binding study using mutants at three positively charged sites in the collagen-like domain reveals that the site of R496 K499 K502 plays the most important role in ligand binding functions for microbes and OxLDL.

Conclusions: CL-P1 has three unique functional domains: the collagen-like domain mainly acts against most negatively charged ligands, and the CRD specifically does against sugar substances, while the coiled-coil domain additionally acts on modified LDL.

General Significance: We considered that the binding activity for various ligands due to the association of a coiled-coil domain, a collagen-like domain and/or a CRD in CL-P1, might play a role in physiological functions in the animal body.

Introduction

Collectin is a superfamily group of c-type lectin, which is characterized by having a carbohydrate recognition domain (CRD) and a collagen-like domain. It can interact with various pathogens from viruses to metazoans, and are thought to be a critical component of the innate immune system (1, 2). Alignment among amino acid sequences of CRDs of various collectins has been observed in a presentation of the six classes of the collectin family: (1) the MBL (mannan-binding protein or lectin) group consisting of MBL, MBL-A, and MBL-C; (2) the SP-A (surfactant protein A) group; (3) the SP-D (surfactant protein D) group consisting of SP-D, bovine CL-43 (collectin 43), CL-46 (collectin 46) and conglutinin; (4) the CL-P1 (collectin placenta 1) group; (5) the CL-L1 (collectin liver 1) group; and (6) the CL-K1 (collectin kidney 1) group (3).

Furthermore, human collectins have been divided into four classes by the phylogenetic tree and their gene localization, which are the classical collectin classes of MBL, SP-A, and SP-D, CL-L1, CL-P1, and CL-K1 group. (4). Like most collectins, a membrane-type collectin CL-P1 also consists of the above two domains, and additionally it contains a long coiled-coil domain, a 27 amino acid transmembrane domain and a 39 amino acid leucine-zipper like motif that exists in the cytoplasmic domain (5). This domain organization of CL-P1 is very similar to scavenger receptor A-I (SR-AI), which has a short intraplasmic domain, a transmembrane domain, a coiled-coil domain, a collagen-like domain and scavenger receptor-cysteine rich domain (SR-CR) (5). Recent genomic analysis demonstrates that CL-P1 has been classified as a SR-A gene of *SCARA4* as well as a collectin gene of *COLEC12* (6). Scavenger receptors are generally expressed in macrophages and vascular smooth muscle cells, which are considered a heterogenous protein family that commonly binds and uptakes various foreign substances and pathogens. The scavenger receptor family has at least eight different subclasses (Class A - Class H) which bear little sequence identity to each other (7). The scavenger receptors expressed in vascular endothelial cells are composed of several protein groups, such as LOX-1 (8), SR-BI (9-11), SREC (12), FEEL-1/stabilin-1 and FEEL-2/stabilin-2 (13), and CL-P1 (5).

We have identified CL-P1 from placental cDNA as a membrane type collectin, which can endocytose and phagocytose Gram-negative and -positive bacteria and yeast as well as oxidized low density lipoprotein (OxLDL) in vascular endothelial cells (5, 14). Usually, collectin can utilize the CRD as a ligand binding domain, and a scavenger receptor of SR-AI can use the polycharged sites in the collagen-like domain, as the domain (15). However, it is unknown with ligand binding domains because CL-P1 has two binding domains of a collagen-like sequence and a CRD. In this study, we constructed seven types of CL-P1 deletion mutants to determine the site of the ligand binding domain, and observed whether the specific binding to sugar ligand, microbes, or oxidized LDL decreases or not in cells with CL-P1 deletion mutants and CL-P1 containing mutations of amino acid, respectively.

Materials and methods

Construction of CL-P1 deletion mutant expression vectors

The cDNA sequence of human CL-P1 was identified and cloned into pcDNA3.1/myc-HisA expression vector (5), and used as template DNA for constructing the CL-P1 mutants presented in this paper (Figure 1). We designed nine primers to amplify each fragment of CL-P1 (Table 1). The C-terminal truncated forms of hCL-P1 deletion mutants named as Δ CRD, Δ col-CRD and Δ cc-col-CRD were amplified using C-terminal primers ON7070, ON7060 and ON7061, respectively, and N-terminal common primer ON7068. Each N- and C- terminal primer contains an additional restriction enzyme site *NotI* and *XbaI*, respectively. The PCR amplified fragments were sub-cloned into pT7Blue T-Vectors (Novagen), and sequencing was performed. The sub-cloned fragments were digested using *NotI/XbaI*, cloned into *NotI/XbaI* digested pcDNA3.1/myc-HisA, and sequencing was performed. CL-P1 Δ col was constructed as described below. CL-P1 Δ col-CRD described above was used for the N-terminal fragment template DNA of Δ col.

There is an internal *AccI* site positioned 1,279 bp from the ATG site at the coiled-coil domain in Δ col-CRD. Primer ON7088 contains part of the coiled-coil domain; from the *AccI* site to the C-terminal end, and the neck domain. Primer set ON7088/ON7069 amplifies part of the coiled-coil, neck and CRD domain. Sub-cloned Δ col-CRD was double digested using *NotI* and *AccI*. The sub-cloned primer set ON7088/ON7069 amplified fragment was likewise double digested using *AccI* and *XbaI*. The two digested fragments were cloned into a *NotI/XbaI* digested expression vector and sequencing was performed.

CL-P1 Δ cc, Δ cc-CRD and Δ cc-col contain common fragments consisting of the cytoplasmic domain, the transmembrane domain and the first seven amino acids counting from the N-terminal of the coiled-coil domain. This fragment was amplified using primer set ON7068/ON7085 which contains an additional restriction enzyme site using *NotI* and *SgrAI*, respectively. The C-terminal fragments of Δ cc, Δ cc-CRD and Δ cc-col were amplified using primer sets ON7086/ON7069, ON7086/ON7070 and ON7087/ON7069, respectively. Each forward primer and reverse primer contains an additional restriction enzyme site *SgrAI* and *XbaI*, respectively. Each of the sub-cloned and sequenced N-terminal and C-terminal fragments were double digested using *NotI/SgrAI* and *SgrAI/XbaI*, respectively, and cloned into expression vectors. All CL-P1 deletion mutant expression vectors were sequenced and purified using EndoFree plasmid maxi kit (QIAGEN) and used for transfection experiments.

Construction of collagen-like domain positively charged cluster mutants

Positively charged cluster mutants, which are versions of CL-P1 where the positively charged clusters of the collagen-like domain are converted into non-charged clusters, were constructed using the QuickChange site-directed mutagenesis kit purchased from QIAGEN. Primer set ON0006/ON0007 was used to convert the three arginines of the first positively charged cluster,

R488 R501 R504, into alanine to construct Col mutant I (Figure 7a). Primer set ON0008/ON0009 was used to convert the three lysines of the middle positively charged cluster, K466 K469 K472, into alanine to construct Col mutant II. Primer sets ON9050/ON9057, ON3009/ON3010 and ON9058/ON9059 were used to alter arginine and two lysines of the last positively charged cluster, R496 K499 K502, into alanine to construct Col mutant III. Col mutant IV was constructed by using all of the above primers to change the nine positively charged amino acids into alanine. Col mutants MWW, WMW and WWM were constructed using primer sets ON3007/ON3008, ON2181/ON2182 and ON3009/ON3010, respectively (Figure 6b). Additionally, all three of these primer sets were used to construct Col mutant MMM. All hCL-P1 collagen-like domain mutant expression vectors were sequenced and purified using EndoFree plasmid maxi kit (QIAGEN) and used for transfection experiments.

Cell culture

CHO/dlA7 cells were grown in Ham's F12 medium (SIGMA) supplemented with 5% heat inactivated Fetal Bovine Serum (GIBCO) at 37°C, 5% CO₂. The third to sixth passage cells were used for all experiments.

Transfection

CHO/dlA7 cells were seeded onto Poly-L-Lysine-Coated 35 mm Glass Based Dishes (IWAKI) prior to transfection. Cells were then transfected with LipofectamineLTX reagent (Invitrogen) according to the manufacturer's procedure. 6 hours after transfection, LipofectamineLTX/plasmid DNA complex solution was replaced with fresh 5% FBS Ham's F12 medium. After an additional 18 hours incubation, transfected cells were immediately used in the ligand binding assays or immunoblotting assays.

Purification and oxidization of LDL

OxLDL was prepared by a modified method of Nishi et al. (16). Blood plasma was obtained by centrifugation at 2,000 rpm for 15 min. The plasma was collected into 4PC tubes (HITACHI) and stratified with 0.25 mM EDTA PBS pH 7.4, then centrifuged at 100,000 rpm for 7 min at 10°C. After removing the creamy top layer, 0.25 mM EDTA PBS pH 7.4 was added and centrifuged at 100,000 rpm for 2 h 30 min at 10°C. After removing the top layer, 0.5 g/ml KBr was added for density gradient centrifugation and centrifuged at 100,000 rpm for 2 h 30 min at 10°C. The LDL top layer was collected and dialyzed with PBS to remove KBr. LDL concentration was determined by using a BCA assay kit (Pierce). LDL was oxidized by incubating with 5 μM CuSO₄ at 37°C for 24 h and oxidization was stopped by addition of EDTA.

Ligand binding assay

Texas-Red conjugated zymosan particle A (*Saccharomyces cerevisiae*), *S. aureus* (wood strain without protein A) BioParticles Fluorescein conjugate, and *E.coli* (K-12 strain) BioParticles Fluorescein conjugate (Molecular probe) were used as microbe ligands. Ligands were diluted in

FBS-Free Ham's F-12 medium to a final concentration of 50 $\mu\text{g/ml}$ (microbes) and 100 $\mu\text{g/ml}$ (zymosan), to be used for ligand binding. Transiently transfected CHO/Id1A7 were washed with PBS, then incubated at 4°C for 30 min with each type of diluted ligand. After incubation, cells were washed with PBS to remove unbound ligands; then fixed with 4% paraformaldehyde PBS at room temperature for 30 min. Cells were immunostained with anti-Myc monoclonal antibody (Invitrogen) followed by Alexa 488 or 594 conjugated goat anti-mouse IgG (Invitrogen) treatment. Hoechst33342 was used for nuclear counterstaining. Fluorescent images of protein expression and ligand binding were observed with an Olympus IX70-23FL/DIC-SP, SPOT2-SP system (Olympus Co. Ltd.) and fluorescence microscope BZ-9000 (KEYENCE). The membrane immunofluorescence (MIF) s of CL-P1 and deletion mutants were analyzed by the fluorescence microscope BZ-9000 and the BZ-HIC program (KEYENCE). The percentage of ligand binding was determined using the number of target protein expressing cells and ligand bound cells. Data are shown as means \pm S.D. of results from three independent experiments. For the sugar ligand binding assay, Lewis-X-PAA-Fluo (GlycoTech) was diluted to a final concentration of 10 $\mu\text{g/ml}$, and its binding ability was tested with the same procedures as the microbe ligand binding assays described above.

For the OxLDL binding assay, OxLDL was also diluted to a final concentration of 10 $\mu\text{g/ml}$ and had its binding ability tested with the modified procedures as the microbe ligand binding assays described above. In the OxLDL binding assay, bound OxLDL was visualized using sheep anti-human ApoB antibody (THE BINDINGSITE) followed by Alexa 594 conjugated donkey anti-sheep IgG. For statistical data analysis, the integrated density ratio of OxLDL (red) and CL-P1 (green) was calculated by using either NIH Image or BZ-HIC program (KEYENCE) to assess the percentage of ligand binding. In the results, values are the mean of three independent experiments; bars \pm SD. **, $p < 0.001$.

Statistical analysis

Statistical analysis was performed using the Student's *t* test included in the *JMP* statistics software package (version 7, SAS). $P < 0.001$ was considered statistically significant.

Immunoblot assay

For immunoblot analysis, cells transiently transfected with hCL-P1 and CL-P1 deletion mutants were collected and suspended in a lysis buffer (50 mM $\text{NaH}_2\text{PO}_4 \cdot 2\text{H}_2\text{O}$, 300 mM NaCl, 10 mM Imidazol, 0.05% Tween 20, pH 8.0). The cells were broken down by sonication and centrifuged to remove cell debris. For the reducing and non-reducing Western blotting condition, cells were separated on a 5-20% gradient gel with and without a 2-mercaptoethanol sample buffer (Wako). For native condition Western blotting, cells were separated on 3-12% Bis-Tris Gel without 2-mercaptoethanol, in a Native-PAGE sample buffer (Invitrogen). The separated samples were transferred to PVDF membranes, and nonspecific binding sites were blocked by incubating the membranes with Block Ace blocking buffer (Dainippon Sumitomo Pharma Co.) for 1 h at 37°C.

Subsequently, the membranes were incubated with anti-Myc monoclonal antibody and HRP-conjugated goat anti-mouse IgG. Luminescence images of the target-bound antibodies were observed using the ECL Plus Western blotting detection kit (Amersham Pharmacia) and LAS-3000 (Fuji Photo Film Co.).

Results

Construction of CL-P1 deletion mutants

In order to identify the functional domain in human CL-P1, we constructed seven different types of CL-P1 deletion mutant (Figure 1). All proteins expressed in the transfected cells were tagged with Myc-epitope so that they could be demonstrated by staining with anti-Myc monoclonal antibody. The cytoplasmic domain of 39 amino acids (I: CD) and the transmembrane domain of 23 amino acids (II: TM) in CL-P1 are conserved in all constructs. CL-P1 is comprised of an extracellular region: a coiled-coil domain (III: cc), a collagen-like domain (IV: col) and neck domain (V) attached to a carbohydrate recognition domain (VI: CRD). The full CL-P1 and seven deletion mutants were CL-P1, Δ CRD, Δ col, Δ col-CRD, Δ cc, Δ cc-CRD, Δ cc-col, and Δ cc-col-CRD.

Expression of CL-P1 deletion mutants in CHO/Idl A7

MIF analysis using anti-Myc antibody demonstrated that CL-P1 and all deletion mutants were expressed on the cell surface (Fig. 2a) except for Δ cc-col-CRD, which is observed after permeabilization treatment only in cytoplasm, but not on the cell surface (Fig. 2a). Δ cc-col-CRD mutant was considered as a negative control for the ligand binding assay, whereas complete CL-P1 was useful as the positive control (5). We performed SDS-PAGE and Western blotting to verify the protein size and amount of each deletion mutant. The hypothetical protein size of non-glycosylated CL-P1 and CL-P1 deletion mutants were deduced as follows: CL-P1, 81 KDa; Δ CRD, 66 KDa; Δ col, 63 KDa; Δ col-CRD, 48 KDa; Δ cc, 40 KDa; Δ cc-CRD, 25 KDa; Δ cc-col, 25 KDa; Δ cc-col-CRD, 7 KDa. Western blotting in the reduced condition showed (Fig. 2b) that complete CL-P1 and deletion mutants appeared as their anticipated sizes with the addition of a glycosylation value (lower bands meaning the size of the protein was not glycosylated). Previously our results showed glycosylated human CL-P1 with almost 140 KDa.as (5). These results mean that a substantial portion of the protein at steady state might be located within the cell in a non-glycosylated form in the ER or Golgi area. To confirm the multimeric structure of CL-P1, proteins were separated by using non-reducing gel detected by Western blotting in Fig. 2b and 2c. Deletion of the CRD or collagen-like domain mutants showed at least two trimer proteins but those of coiled-coil domain showed one trimer in non-reducing SDS-PAGE (Fig. 2b, c). These results indicate that CL-P1 and deletion mutants with a non-glycosylated form as well as a glycosylated one might also make a trimeric structure in the ER or Golgi and the cell surface. The cell surface expression of CL-P1 and deletion mutants might be important in supporting their binding ability. The intensity of the MIF in the supplemental figure 2 demonstrated that the cell surface expression level (%) in deletion mutants except for Δ cc-col-CRD showed the wide range from 14 - 95%, compared to that of CL-P1. However, later binding analyses in Fig. 3 and 4b, c, d in Δ cc, Δ cc-CRD and Δ cc-col deletion mutants indicate that the cell surface expressions in those mutants might be sufficient level to support their binding activities in those in a transient transfection study.

Carbohydrate recognition domain (CRD) in CL-P1 interacts with LewisX antigen

The CRD of CL-P1 contains a Galactose type binding motif (Gln-Pro-Asp), but does not contain mannose and glucose types (Glu-Pro-Asn). The glycan array and structural analysis demonstrated that the CRD in CL-P1 had a high specific binding activity against a LewisX antigen, also known as SSEA-1, which contains a galactose β 1, 4 (fucose α 1, 3) N-acetyl-glucosamine (Gal β 1, 4 (Fuc α 1, 3) GlcNAc-R) (17). To analyze the binding domain of CL-P1 to the LewisX antigen on living cells, we used CHO/Id1A7 transiently expressing full CL-P1 and CL-P1 deletion mutants. The results of Figure 3 and Table 1 showed that CL-P1 mutants without the CRD could not interact with LewisX (green color). The merged figures with yellow color indicate that the bindings to LewisX are observed in cells expressing the CRD protein. Therefore, CL-P1 proves itself to be a membrane type collectin, which recognizes and interacts with sugar antigens due to the CRD.

Collagen-like domain in CL-P1 recognizes mainly microbial and fungal ligands

We previously reported that CL-P1 can interact with several species of bacteria and yeast (5). In this study, the immunofluorescence labeled BioParticles of Gram positive bacteria (*S. aureus*), Gram negative bacteria (*E. coli*) and fungus (zymosan) were used as microbial ligands. As shown in Figure 4a and Table1, FITC-labeled *E. coli* failed to bind the collagen-like domain deletion mutants of Δ col, Δ col-CRD, Δ cc-col and Δ cc-col-CRD mutants.

Quantitative analyses of the binding of *E. coli*, *S. aureus*, and zymosan to those cells were performed by calculating the ratio of CL-P1 expressing cells and ligand bound cells. The statistical analysis in Figure 4b and 4c revealed that the binding efficiency in Δ col, Δ col-CRD, Δ cc-col and Δ cc-col-CRD mutants against *E. coli* and *S. aureus* significantly decreased compared with the binding efficiency in complete CL-P1 cells, to 14.7%, 21.4%, 5.4%, 5.5% and 4.20%, 0.48%, 2.08%, 0.78%, respectively ($p < 0.0001$). There were no significant differences between those bindings of Δ col, Δ col-CRD, Δ cc-col and the negative control Δ cc-col-CRD ($p = 0.28, 0.07, 0.98,$ and $p = 0.52, 0.75$ and $0.94,$ respectively). Furthermore, we confirmed no significant difference of binding efficiencies to *E. coli* and *S. aureus* between CL-P1 and the CRD deletion mutant. These results indicate that CL-P1 can recognize and interact with *E. coli* and *S. aureus* not through its CRD but through its collagen-like domain (Table 1).

The binding ability with Texas red-labeled zymosan among Δ col, Δ col-CRD, Δ cc-col and Δ cc-col-CRD mutants showed a low level of 19.9%, 11.5%, 20.1% and 11.2%, respectively ($p < 0.0001$, Figure 4d). Interestingly, the binding ability significantly decreased with zymosan in the CRD deletion mutant compared with complete CL-P1, 64.0% ($p < 0.001$). Furthermore, there is no significant decrease of its binding in mutants with deleted coiled-coil domain ($p = 0.0013$), rather, the binding efficiency increased compared to that of complete CL-P1 (123.4%). Therefore, it may be a possibility that the coiled-coil domain could act as a binding inhibitor (Table 1).

Oxidized LDL interacts with CL-P1 in partially different mechanisms from microbial ligands

CL-P1 can only interact with oxidized LDL (OxLDL), not native LDL or acetylated LDL (5). OxLDLs are considered to be most active in interactions among endothelial cells (EC), macrophages, and smooth muscle cells, and have been implicated in the development of atherosclerosis (18, 19). Figures 5a and 5b showed that the binding abilities of deletion mutants Δ col or Δ cc demonstrated a similar low level of 18.2% and 21.4%, and there was no significant difference, compared with that of Δ cc-col-CRD as the negative control. These results indicate that the coiled-coil domain as well as the collagen-like domain is mainly involved in interaction with OxLDL, although the mechanism is unknown. Our binding analysis with CL-P1 and microbes suggests that an α -helical coiled-coil structure is not important for binding ability in comparison with a collagen-like domain (Figure 4 and Table 1). However, the binding analysis with CL-P1 and OxLDL in Fig. 5 demonstrated that CL-P1 mutants deleted a coiled-coil domain and still retain the binding activity to microbes, but fail to interact with OxLDL.

The positively charged clusters play an important role in ligand bindings

We found positively charged clusters in the collagen-like domain in human CL-P1 and bovine SR-AI as shown in Figure 6a. The SR-AI has one cluster containing three lysine residues (K334 K337 K340) in position 334, 337 and 340 in the collagen-like domain. This basic amino acid cluster in SR-AI is considered to be the ligand binding domain (15). It has been reported that the middle lysine residue of positively charged cluster, K337, was essential for ligand binding (Fig. 6a). Furthermore, there are three positively charged clusters (R448 R451 R454, K466 K469 K472 and R496 K499 K502) in the collagen-like domain in human CL-P1, consisting of lysine or arginine which shows positive electric charge (Fig. 6a). These three positively charged clusters in the collagen-like domain in CL-P1 are evolutionarily conserved in human, bovine, mouse, rat and chicken species (Figure 8). In addition, lower animals such as frogs and zebrafish have at least two positively charged clusters in their collagen-like domains.

Based on a previous report, we altered the middle positively charged amino acid of each cluster, R451, K469 or K499, into alanine to form three types of mutants (M) (MWW, WMW, and WWM) and changed all three basic amino acids into alanine (MMM) in Figure 6b (15). CHO/IdIA7 was transiently transfected with CL-P1 mutants containing the above mutations of the collagen-like domain, then the binding assay was performed using FITC-labeled *E. coli* or OxLDL. The binding efficiencies with FITC-labeled *E. coli* in all mutants, MWW, WMW, WWM, and MMM, were 96.7%, 93.7%, 87.3% and 84.7%, respectively (Fig. 6c). Likewise, those with OxLDL in the same mutants showed 99.2%, 99.8%, 85.4% and 81.2%, respectively (Fig. 6d). These results indicated that there is no significant statistical difference between four mutants including MMM and hCL-P1 with the binding to *E. coli* or OxLDL. Next, we changed all positively charged amino acids of one cluster into alanine to construct Col mutant I, II and III, and changed all positively charged amino acids of all clusters into alanine to construct Col mutant IV (Fig. 7a).

However, the immunoblot analysis in Supplemental Figure 3 demonstrated that those four mutants could produce solid proteins and make oligomeric structures similar to CL-P1. Furthermore, MIF indicates that all mutants expressed on the cell surface as shown in Fig.7b-I and 7c-I, and in Supplemental Figure 4. The binding activities with FITC-labeled *E. coli* in Col mutant III and IV significantly decreased to 20.0% and 23.3%, respectively, $p < 0.0001$ (Fig. 7b-I, II). There was no significant difference in the binding ability of Col mutants III and IV, $p = 0.85$. Finally, the binding activities with OxLDL in Col mutant III and IV, decreased to 44.3% and 31.6% respectively ($p < 0.0001$), and there was no significant difference between Col mutant III and IV (Fig. 7c-I, II). These results indicate that the third positively charged cluster of R496 K499 K502 in the collagen-like domain can have a critical role in ligand binding with microbes as well as modified LDL. In addition, the second positively charged cluster might be partially involved in binding to both ligands.

Discussion

Collectins are composed of four structural domains: an N-terminal cysteine-rich domain, a collagen-like domain, a hydrophobic neck domain, and a CRD (Fig. 1). Collectins bind to oligosaccharide repeat patterns on the surface of microorganisms through the CRD and act as a pattern-recognition receptor in a calcium ion dependent manner (20, 21). The membrane-type collectin CL-P1 also retains a long coiled-coil domain as the candidate of the third functional domain (Fig. 1). It is necessary for collectins to form a trimeric form, because it is the minimal subunit that can allow collectins to bind their various ligands with high affinity (22, 23). The langerin, which is a C-type membrane type lectin expressed on Langerhans cells, must be in a trimeric structure to be able to bind to a ligand through the CRD (24). It has also been demonstrated that the disruption of the trimeric form in SP-D causes a remarkable reduction in its affinity with ligands (25).

The trimeric structure in a collectin protein is created by a collagen-triple helix structure in a collagen-like domain. Even without the collagen-like domain, bovine conglutinin can hold less viral inhibition activity and conglutination activity since the neck domain can make a trimeric form. Therefore we designed deletion mutants, all of which have a neck domain. Using Western blotting, we confirmed the structures of the mutants. All deletion mutants produced solid proteins except for Δ cc-col-CRD and they existed as a multimeric form (Fig. 2b, c). The MIF analyses in Figure 2a and Supplemental figure 2 and the later binding analyses in Fig. 3 and 4b, c, d in Δ cc, Δ cc-CRD and Δ cc-col deletion mutants also indicate that the complete CL-P1 and deletion mutants were expressed on the cell surface so that they might be able to bind various ligands.

In pulmonary collectin, SP-A and SP-D have mannose/maltose/fucose-recognizing type CRD (Glu-Pro-Ans/Ala) and bind to a broad range of carbohydrates which have been defined with their massive number of microbial targets (22, 26, 27). It has been characterized that the CRD in SP-D has been bound to sugar epitopes in influenza A virus by using monoclonal antibody (28). The CRD in MBL interacts with the vicinal equatorial hydroxyl group of mannose, N-acetylglucosamine and fucose (29, 30). Unlike most collectins, CL-P1 has a galactose-recognizing type CRD (Gln-Pro-Asp) which was originally shown by a truncated type CL-P1 (31). In a previous study, the deletion mutant of the CRD in SR-CL showed that its binding ability was not changed when acted on by *E. coli* (32).

Coombs et al. identified that CL-P1 interacted with carbohydrate epitope LewisX with high specificity (17). They performed a Glycan array analysis using the CRD protein expressed in prokaryote cells. In our study, we analyzed the binding domain in CL-P1 expressed on CHO cells to LewisX, and identified that the CRD was a functional domain recognizing LewisX (Figure 3). Additionally, it was found that the deletion mutants of the CRD led to less binding to zymosan (Fig. 4d), since a cell wall extract of yeast is composed of numerous β -glucan and α -mannan. It suggests

that the CRD can assist the binding between the collagen-like domain in CL-P1 and zymosan (Fig. 4d). However, the deletion of the CRD could not significantly reduce the binding ability to bacteria and oxidized LDL, in Fig. 4b, c and Fig. 5a, b. These results indicate that the CRD in CL-P1 is not the major binding domain to microbes and oxidized LDL (Table 1) although collectin in general uses the CRD as a ligand binding domain for bacteria or viruses.

On the other hand, the collagen-like domain contains a Gly-X-Y repeat motif in which frequently, X occupies proline and Y occupies hydroxyproline. Ligand binding analysis using the C-terminal deletion mutants in bovine SR-AI revealed that 22 amino acids at the C-terminal portion of the collagen-like domain are crucial for ligand binding and endocytosis (15). Of these 22 amino acids, amino acid number 334, 337 and 340 corresponded to the Y amino acid residue of Gly-X-Y, respectively, and was a positively charged amino acid of lysine. The comparison of the amino acid sequences among human, bovine, rabbit, and mouse SR-AI showed that the collagen-like domain was highly conserved and ten amino acid sequences containing three lysine residues (K334 K337 K340) were identical (33). Although SR-AI has only one positively charged cluster in the collagen-like domain, there are three positively charged clusters in that of CL-P1 (Fig. 6a). As shown in Fig. 8, these three positively charged clusters are well conserved from fish to humans. Even in amphibian and fish living in different environments, two of three positively charged clusters in their collagen domains are completely conserved. Additionally, Table 2 demonstrates that all amino acid sequences in the collagen-like domain among animals are more highly conserved than those of other extracellular domains. These results indicate that the high conservation of genetic identity in the collagen-like domain in CL-P1 in vertebrates, might play any important role in physiological functions.

The point mutations in SR-AI which converted these lysine residues to alanine residues as an uncharged amino acid residue, dramatically decreased the binding activity to acetylated LDL and oxidized LDL (15). Doi et al. suggested that, K337, the middle lysine residue of the positively charged cluster (K334 K337 K340), was crucial for ligand binding (15). When the middle positively charged amino acid in the cluster in CL-P1 was converted into alanine in four mutants, their binding activities with bacteria and OxLDL did not significantly decrease (Fig. 6b, c and d). Next, we changed all positively charged amino acids of one cluster or all clusters into alanine to construct Col mutant I, II, III, or mutant IV (Fig. 7a). The binding activities with bacteria and OxLDL in Col mutant III and IV, significantly decreased, respectively (Fig. 7b, c). These results indicate that the presence of at least one complete positive cluster is needed and the third positively charged cluster of R496 K499 K502 is important in retaining the ligand binding activity with microbes and modified LDL.

Recently, Fukuda et al. revealed that zebrafish CL-P1 (zCL-P1) transfected cells could bind and endocytose bacteria and fungi as did human CL-P1 (34). Knockdown analysis

demonstrated that the fish embryos had severe morphological abnormalities such as short body length and defects in the dorsal aorta (34). These results suggest that zCL-P1 plays a role in body development during the early embryogenic stage in fish. Complement factor 1q (C1q) is another collectin-like protein: knockout mice manifested increased frequency of fetal resorption, reduced fetal weight, and smaller litter sizes compared with wild-type mice (35). These two results suggest that CL-P1 and C1q might be involved in embryogenesis and maintaining a healthy pregnancy, although it is unknown in the molecular mechanism. Very recently, Degn and Thiel suggest that CL-P1 might be able to activate the complement pathway, since the CL-P1 molecule might have a MASP binding site in a collagen-like domain (36). However, SR-AI has no MASP binding site in the collagen-like domain. Additionally, the KO mice in SR-AI have normal delivery and exhibit the normal phenotype. CL-P1 and SR-AI belong to the same scavenger gene family but their biological functions in the embryonic stage might be different. The reason considered was because CL-P1 has various functional domains different from SR-AI. The CRD can recognize the sugar ligand as LewisX, the collagen-like domain can bind MASP as well as microbes and OxLDL, and the coiled-coil domain can interact with OxLDL. Assumed and unique activities might be mediated to a particular and unexpected function. Definitive mechanisms or related molecules are at this time, unknown. Further investigations are needed in order to understand the mechanisms of biological functions in CL-P1.

References

1. Runza, V. L., Schwaeble, W, Mannel, D. N. Ficolins: Novel pattern recognition molecules of the innate immune response. *Immunobiology* 213 (2008) 297- 306.
2. Kilpatrick, D. C. Mannan-binding lectin and its role in innate immunity. *Transfusion Medicine* 12 (2002) 335- 351.
3. Ohtani, K., Suzuki, Y., Wakamiya, N. Biological functions of the novel collectins CL-L1, CL-K1, and CL-P1, *J. Biomed. Biotechnol.* 2012 (2012) 493945.
4. Ohtani, K., Suzuki, Y., Wakamiya, N. New aspects of collectin functions. *Glycoscience: Biology and Medicine.* in press.
5. Ohtani, K., Suzuki, Y., Eda, S., Kawai, T., Kase, T., Keshi, H., Sakai, Y., Fukuoh, A., Sakamoto, T., Itabe, H., Suzutani, T., Ogasawara, M., Yoshida, I., Wakamiya, N. The membrane-type collectin CL-P1 is a scavenger receptor on vascular endothelial cells. *J. Biol. Chem.* 276 (2001) 44222-44228.
6. <http://www.genenames.org/genefamilies/COLEC>
7. Greaves, D. R., Gough, P. J., and Gordon, S. Recent progress in defining the role of scavenger receptors in lipid transport, atherosclerosis and host defence. *Curr. Opin. Lipidol.* 9 (1998) 425-432.
8. Sawamura, T., Kume, N., Aoyama, T., Moriwaki, H., Hoshikawa, H., Aiba, Y., Tanaka, T., Miwa, S., Katsura, Y., Kita, T., and Masaki, T. An endothelial receptor for oxidized low-density lipoprotein. *Nature* 386 (1997) 73-77.
9. Acton, S. L., Scherer, P. E., Lodish, H. F., Krieger, M. Expression cloning of SR-BI, a CD36-related class B scavenger receptor. *J. Biol. Chem.* 269 (1994) 21003-21009.
10. Yuhanna, I. S., Zhu, Y., Cox, B. E., Hahner, L. D., Osborne-Lawrence, S., Lu, P., Marcel, Y. L., Anderson, R. G., Mendelsohn, M. E., Hobbs, H. H., and Shaul, P. W. High-density lipoprotein binding to scavenger receptor-BI activates endothelial nitric oxide synthase. *Nat. Med.* 7 (2001) 853-857.
11. Li, X. A., Titlow, W. B., Jackson, B. A., Giltaiy, N., Nikolova-Karakashian, M., Uittenbogaard, A., and Smart, E. J. High density lipoprotein binding to scavenger receptor, Class B, type I activates endothelial nitric-oxide synthase in a ceramide-dependent manner. *J. Biol. Chem.* 277 (2002) 11058-11063.
12. Adachi, H., Tsujimoto, M., Arai, H., and Inoue, K. Expression cloning of a novel scavenger receptor from human endothelial cells. *J. Biol. Chem.* 272 (1997) 31217-31220.
13. Sørensen, K. K., McCourt, P., Berg, T., Crossley, C., Le Couteur, D., Wake, K., Smedsrød, B. The scavenger endothelial cell: a new player in homeostasis and immunity. *Am. J. Physiol. Regul. Integr. Comp. Physiol.* 303 (2012) R1217-1230.
14. Jang S., Ohtani K., Fukuoh A., Yoshizaki T., Fukuda M., Motomura W., Mori K., Fukuzawa J., Kitamoto N., Yoshida I., Suzuki Y., and Wakamiya N. Scavenger receptor collectin placenta 1

- (CL-P1) predominantly mediates zymosan phagocytosis by human vascular endothelial cells. *J. Biol. Chem.* 284 (2009) 3956-3965.
15. Doi, T., Higashino, K., Kurihara, Y., Wada, Y., Miyazaki, T., Nakamura, H., Uesugi, S., Imanishi, T., Kawabe, Y., Itakura, H., Yazaki, Y., Matsumoto, A., Kodama, T. Charged collagen structure mediates the recognition of negatively charged macromolecules by macrophage scavenger receptors. *J. Biol. Chem.* 268 (1993) 2126-2133.
 16. Nishi, K., Itabe, H., Uno, M., Kitazato, K. T., Horiguchi, H., Shinno, K., Nagahiro, S. Oxidized LDL in carotid plaques and plasma associates with plaque instability. *Arterioscler. Thromb. Vasc. Biol.* 22 (2002) 1649-1654.
 17. Coombs, P. J., Graham, S. A., Drickamer, K., Taylor, M. E. Selective binding of the scavenger receptor C-type lectin to LewisX trisaccharide and related glycan ligands. *J. Biol. Chem.* 280 (2005) 22993-22999.
 18. Larkin, J. M., Brown, M. S., Goldstein, J. L., and Anderson, R. G. Depletion of intracellular potassium arrests coated pit formation and receptor-mediated endocytosis in fibroblasts. *Cell* 33 (1983) 273-285.
 19. Steinberg, D. Low density lipoprotein oxidation and its pathobiological significance. *J. Biol. Chem.* 272 (1997) 20963-20966.
 20. Weis, W. I., Grichlow, G. V., Murthy, H. M. K., Hendrickson, W. A., Drickamer, K. Physical characterization and crystallization of the carbohydrate-recognition domain of a mannose-binding protein from rat. *J. Biol. Chem.* 266 (1991) 20678-20686.
 21. Weis, W. I., Drickamer, K., Hendrickson, W. A. Structure of a C-type mannose-binding protein complex with an oligosaccharide. *Nature* 360 (1992) 127-134.
 22. Ogasawara, Y., Voelker, D. R. The role of the amino-terminal domain and collagenous region in the structure and function of rat surfactant protein D. *J. Biol. Chem.* 270 (1995) 19052-19058.
 23. Vuk-Pavlovic, Z., Standing, J. E., Crouch, E. C., Limper, A. H. Carbohydrate recognition domain of surfactant protein D mediates interactions with pneumocystis carinii glycoprotein A. *Am. J. Respir. Cell Mol. Biol.* 24 (2001) 475-484.
 24. Feinberg, H., Powlesland, A. S., Taylor, M. E., Weis, W. I. Trimeric structure of langerin. *J. Biol. Chem.* 285 (2010) 13285-13293.
 25. Kishore, U., Wang, J-Y, Hoppe, H-J., Reid, K. B. M. The alpha-helical neck region of human lung surfactant protein D is essential for the binding of the carbohydrate recognition domains to lipopolysaccharide and phospholipids. *Biochem. J.* 318 (1996) 505-511.
 26. Haurum, J. S., Thiel, S., Haagsman, H. P., Laursen, S. B., Larsen, B., Jensenius, J. C. Studies on the carbohydrate-binding characteristics of human pulmonary surfactant-associated protein A and comparison with two other collectins: mannan-binding protein and conglutinin. *Biochem. J.* 293 (1993) 873- 878.

27. Clark, H. W., Reid, K. B. M., Sim, R. B. Collectins and innate immunity in the lung. *Microbes and infection* 2 (2000) 273-278.
28. Hartshorn, K., Chang, D., Rust, K., White, M., Heuser, H., Crouch, E. Interactions of recombinant human pulmonary surfactant protein D and SP-D multimers with influenza A. *Am. J. Physiol.* 271 (1996) L753-L762.
29. Lee, R. T., Ichikawa, Y., Fay, M., Drickamer, K., Shao, M-C., Lee, Y. C. Ligand- binding characteristics of rat serum-type mannose- binding protein (MBP-A). *J. Biol. Chem.* 266 (1991) 4810-4815.
30. Weiss, W. I., Kahn, R., Fourme, R., Drickamer, K., Hendrickson, W. A. Structure of the calcium-dependent lectin domain from a rat mannose-binding protein determined by MAD phasing. *Science* 254 (1991) 1608-1615.
31. Yoshida, T., Tsuruta, Y., Iwasaki, M., Yamane, S., Ochi, T., Suzuki, R. SRCL/CL-P1 recognizes GalNAc and a carcinoma-associated antigen, Tn antigen. *J. Biochem.* 133 (2003) 271-277.
32. Nakamura, K., Funakoshi, H., Miyamoto, K., Tokunaga, F., Nakamura, K. Molecular cloning and functional characterization of a human scavenger receptor with c-type lectin (SRCL), a novel member of a scavenger receptor family. *Biochem. Biophys. Res. Commun.* 280 (2001) 1028-1035.
33. Wada, Y., Doi, T., Matsumoto, A., Asaoka, H., Honda, M., Hatano, H., Emi, M., Naito, M., Mori, T., Takahashi, K., Nakamura, H., Itakura, H., Yazaki, Y., Kodama, T. Structure and function of macrophage scavenger receptors. *Ann. N. Y. Acad. Sci.* 748 (1995) 226-239.
34. Fukuda, M., Ohtani, K., Jang, S-J., Yoshizaki, T., Mori, K., Motomura, W., Yoshida, I., Suzuki, Y., Kohgo, Y., Wakamiya, N. Molecular cloning and functional analysis of scavenger receptor zebrafish CL-P1. *Biochim. Biophys. Acta* 1820 (2011) 1150-1159.
35. Agostinis, C., Bulla, R., Tripodo, C., Gismondi, A., Stabile, H., Bossi, F., Guarnotta, C., Garlanda, C., De Seta, F., Spessotto, P., Santoni, A., Ghebrehiwet, B., Girardi, G., Tedesco, F. An alternative role of C1q in cell migration and tissue remodeling: contribution to trophoblast invasion and placental development. *J. Immunol.* 185 (2010) 4420-4419.
36. Degn, S.E., Thiel, S. Humoral pattern recognition and the complement system. *Scand. J. Immunol.* 78 (2013) 181-193.

Acknowledgements

*This work was supported by grants from Grants-in-Aid for Scientific Research (22390113, 26293124) and from the “Knowledge Cluster Initiative” (Sapporo Biocluster Bio-S), a project of the Japan of Ministry of Education, Culture, Sports, Science, and Technology. This work was also supported by grants from Fuso Pharmaceutical Industries, Ltd., the Smoking Research Foundation, the Takeda Science Foundation, and the Mizutani foundation for glycoscience.

Table-1

Summary of binding domains.

Comparison of the binding abilities of CL-P1 deletion mutants and indications of the collagen-like domain with positively charged clusters exhibiting the major binding activity for ligands.

Table-2

Comparison of amino acid sequences in each domain in animal CL-P1s.

Human (*Homo sapiens*), bovine (*Bos taurus*), mouse (*Mus musculus*), rat (*Rattus norvegicus*), chicken (*Gallus gallus*), frog (*Xenopus tropicalis*) and zebrafish (*Danio rerio*) CL-P1 amino acid homology of each domain.

Figure legends

Figure 1. Schematic structure of human CL-P1 and CL-P1 deletion mutants.

CL-P1 is comprised of six domains: I, cytoplasmic domain (CD); II, transmembrane domain (TM); III, coiled-coil domain; IV, collagen-like domain; V, neck domain; VI, carbohydrate recognition domain (CRD). Various mutants lacking one or more of the extracellular domains were constructed. CL-P1 and CL-P1 deletion mutants demonstrated CL-P1: a complete protein, Δ CRD: deletion of CRD, Δ col: deletion of collagen-like domain, Δ col-CRD: deletion of collagen domain and CRD, Δ cc: deletion of coiled-coil domain, Δ cc-CRD: deletion of coiled-coil domain and CRD, Δ cc-col: deletion of coiled-coil domain and collagen domain and Δ cc-col-CRD: deletion of coiled-coil domain, collagen domain and CRD. CD and TM were conserved in all constructs. All proteins were expressed as Myc-epitope tagged fusion proteins.

Figure 2. Analysis of cellular expression patterns in immunocytochemistry staining and structural patterns in SDS-PAGE and Western blotting in CL-P1 and CL-P1 deletion mutants.

(a) CHO/Id1A7 cells were transiently transfected by complete CL-P1 and deletion mutant expression vectors. Membrane immunofluorescence (MIF) staining by anti-Myc murine monoclonal antibody following goat anti-mouse conjugated IgG Alexa 488 reveals that all deletion mutants, except Δ cc-col-CRD, were expressed on the cell surface as type-II membrane proteins. Δ cc-col-CRD mutant was stained only after permeabilization treatment, using the same antibodies as described above (b, c) CHO/Id1A7 cells were transiently transfected by complete CL-P1 and deletion mutant expression vectors. Reduced and non-reduced condition SDS-PAGE following Western blotting using an anti-Myc antibody revealed each deletion mutant to be of the following sizes; CL-P1: about 140 and 84 KDa, Δ CRD: 120 and 76 KDa, Δ col: 110 and 72 KDa, Δ col-CRD: 76 and 62 KDa, Δ cc: 44 KDa, Δ cc-CRD: 34 and 28 KDa, Δ cc-col: 32 and 26 KDa and Δ cc-col-CRD: 15 KDa. Larger sizes than those two sizes in CL-P1 and deletion mutants were considered as glycosylated forms.

Figure 3. CL-P1 interacts with sugar antigen LewisX through the CRD.

CHO/Id1A7 cells transiently transfected by CL-P1 and CL-P1 deletion mutants were incubated with Lewis-X-PAA-Fluo for 30 min at 4°C and fixed with 4% paraformaldehyde (middle, green). The cells were immunostained with anti-Myc antibody followed by Alexa 594 conjugated goat anti-mouse IgG (left, red). Nuclear were counterstained with Hoechst33342 in merged figures. However, Δ cc-col-CRD mutant was stained only after permeabilization treatment, using the same antibodies as described above. Fluorescent images of expressed proteins and Lewis-X were visualized with the Olympus IX70-23FL/DIC-SP, SPOT2-SP system.

Figure 4. CL-P1 mainly interacts with microbial ligands through its collagen-like domain.

(a) The binding images of FITC-labeled *E. coli* (green) in transiently expressed CL-P1 and CL-P1 deletion mutant cells (red). Blue spots indicate Hoechst33342 nuclear staining. *E. coli* bindings are observed in CL-P1 and deletion mutants holding the collagen-like domain. Fluorescent images of CL-P1 proteins and FITC-labeled *E. coli* were visualized with the KEYENCE fluorescence microscope, BZ-9000. (b) The ligand binding efficiency with gram negative bacteria (*E. coli*). The binding efficiency of CL-P1 was shown as 100%. Binding efficiencies with *E. coli* significantly decreased in collagen-like domain deletion mutants (Δcol , $\Delta\text{col-CRD}$, $\Delta\text{cc-col}$ and $\Delta\text{cc-col-CRD}$). (c) The ligand binding efficiency with gram positive bacteria (*S. aureus*). Like *E. coli*, the binding efficiencies significantly decreased in similar deletion mutants. (d) The ligand binding efficiency with fungal ligand (zymosan). The binding character with zymosan dependent on a collagen-like domain was also observed. In addition, the binding efficiency decreased in the CRD deletion mutant (ΔCRD), compared with CL-P1 (CL-P1). The percentage of ligand binding efficiency was calculated using the numbers of target protein expressing cells and ligand bound cells. Data are means \pm S.D. of three independent experiments. The *P* values were calculated relative to two compared values, $**P < 0.001$.

Figure 5. CL-P1 interacts with OxLDL in different mechanisms than with microbial ligands.

(a) The binding image of OxLDL in CL-P1 and CL-P1 deletion mutant cells. The CL-P1 proteins were detected using anti-Myc antibody followed by Alexa488 conjugated goat anti-mouse IgG (left, green), and the bound OxLDL was visualized using sheep anti-human ApoB antibody followed by Alexa594 conjugated donkey anti-sheep IgG (middle, red). Blue spots indicate counterstained nuclear. Fluorescent images of expressed proteins and OxLDL were visualized with the KEYENCE fluorescence microscope, BZ-9000. The positive bindings were observed in CL-P1 and the CRD deleted mutants (b) The binding efficiencies with OxLDL in deletion mutants when the binding efficiency of CL-P1 was shown as 100%. The binding efficiencies in mutants with a deleted coiled-coil domain as well as a collagen-like domain (Δcol , $\Delta\text{col-CRD}$, Δcc , $\Delta\text{cc-col}$, $\Delta\text{cc-CRD}$), significantly decreased, although we observed the full bindings in CL-P1 and CRD-deleted mutants (CL-P1 and ΔCRD). The percentage of ligand binding efficiency was calculated by using the integrated densities of OxLDL (red) and CL-P1 (green). Data are means \pm S.D. of three independent experiments. **, $p < 0.001$.

Figure 6. The middle amino acid in positively charged clusters in the collagen-like domain in human CL-P1 as bovine SR-AI cannot regulate the ligand binding with microbe and modified LDL.

(a) A comparison of positively charged clusters in the collagen-like domain of human CL-P1 (hCL-P1) and bovine SR-AI. There are three positively charged clusters in the collagen-like domain,

R448 R451 R454, K466 K469 K472 and R496 K499 K502, in hCL-P1, and there is one positively charged cluster, K334 K337 K340, in the collagen-like domain in bovine SR-AI, according to their amino acids and locations. (b) The middle amino acid (wild (W), R451, K469 or K499) in positively charged clusters in hCL-P1 was altered into alanine to make mutation (M) (MWW, WMW, and WWM). MMM was constructed by changing all three middle positive amino acids into alanine. (c) The binding efficiency with gram negative bacteria (*E. coli*) in positively charged cluster mutants. These mutations could not affect the binding efficiency. (d) The binding efficiency with OxLDL in positively charged cluster mutants. These mutations could also not affect the binding efficiency. Data are means \pm S.D. of three independent experiments. There is no significant statistical difference between MMM and hCL-P1 with the binding to *E.coli* or OxLDL.

Figure 7. The positively charged clusters in the collage-like domain in human CL-P1 play an important role in mediating the ligand binding with microbe and modified LDL.

(a) Construction of positively charged cluster mutants, having changed all positive charged amino acids of each cluster into alanine to make Col mutant I, II and III, and changed all positive charged amino acids into alanine to make Col mutant IV. (b) I: The binding image of FITC-labeled *E. coli* (middle, green), CL-P1 protein (upper, red), and merged image (lower) in positively charged cluster mutants of Col mutant I, II III, and Col mutant IV. Fluorescent images were visualized with the KEYENCE fluorescence microscope, BZ-9000. II: The binding efficiency with FITC-labeled *E. coli* with the same Col mutants I, II III, and Col mutant IV. The binding efficiencies significantly decreased in Col mutant II, III and IV compared to hCL-P1 ($p < 0.001$). (c) I: I: The binding image of DiI-OxLDL (middle, red), CL-P1 protein (upper, green), and merged image (lower) in positively charged cluster mutants of Col mutant I, II III, and Col mutant IV. Fluorescent images were visualized with the same microscope. II: The binding efficiency with DiI-OxLDL in several mutants. The binding efficiencies significantly decreased in Col mutant II, III and IV compared to hCL-P1 ($p < 0.001$). Data are means \pm S.D. of three independent experiments. Asterisks indicate the statistical significance ($p < 0.001$) against hCL-P1, using the *t*-test.

Figure 8. A comparison of positively charged clusters in the collagen-like domain of CL-P1 among several animal species.

A schematic diagram of the positively charged clusters in the collagen-like domain of human (*Homo sapiens*), bovine (*Bos taurus*), mouse (*Mus musculus*), rat (*Ruttus norvegicus*), chicken (*Gallus gallus*), frog (*Xenopus tropicalis*) and zebrafish (*Danio rerio*) CL-P1. The three positively charged clusters are evolutionally conserved from human to chicken. Frog and zebrafish have two of the three positively charged clusters.

Table 1

	Lewis-X	<i>E. coli</i>	<i>S. aureus</i>	Zymosan	OxLDL
CL-P1	++	++	++	++	++
Δ CRD	-	++	++	+	++
Δ col	++	-	-	-	-
Δ col-CRD	-	-	-	-	-
Δ cc	++	++	++	+++	-
Δ cc-CRD	-	++	++	++	-
Δ cc-col	++	-	-	-	-
Δ cc-col-CRD	-	-	-	-	-

Table 2

		human	bovine	mouse	rat	chicken	frog	zebrafish
I	cytoplasmic	100	94	94	100	100	100	79
II	trasmembrane	100	100	95	95	91	91	82
III	coiled-coil	100	97	91	92	80	69	49
IV	collagen-like	100	93	95	95	83	71	61
V	neck	100	82	82	82	64	34	24
VI	CRD	100	76	87	89	71	63	54
whole protein		100	92	92	92	80	70	53

Figure 1

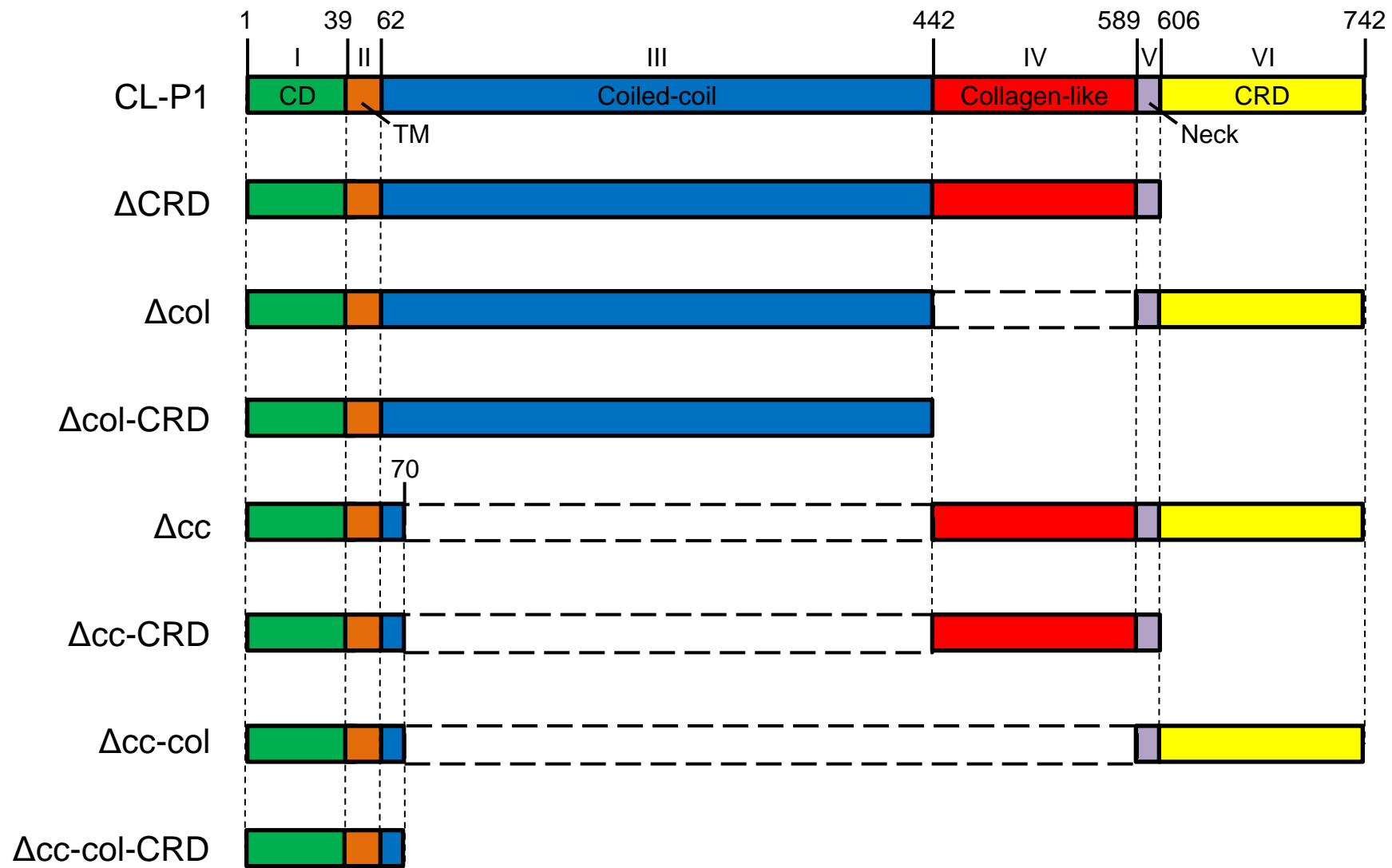


Fig 2 (a)

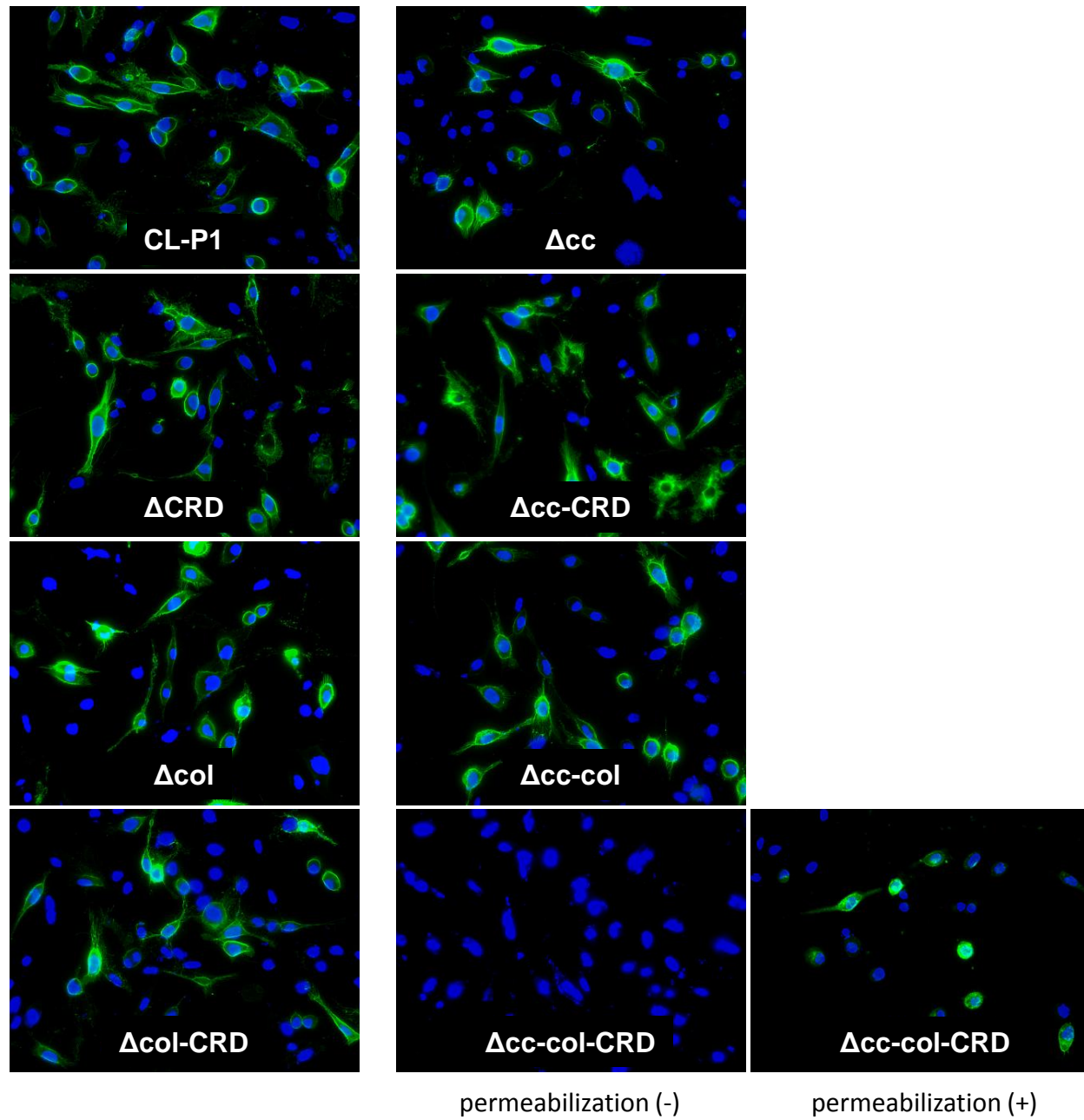


Fig 2 (b)

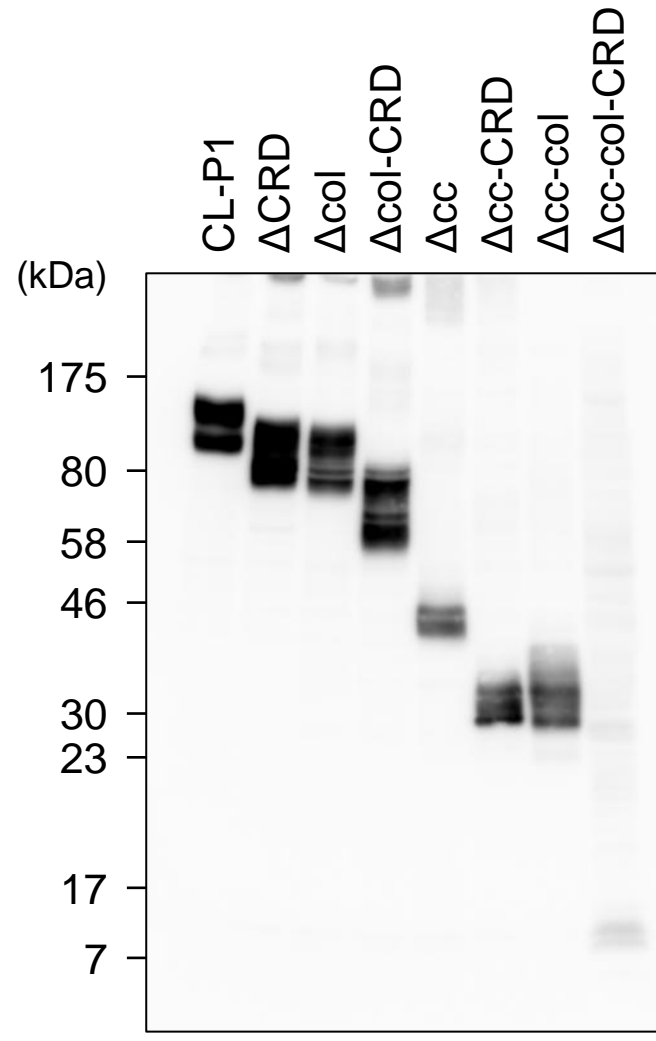


Fig 2 (c)

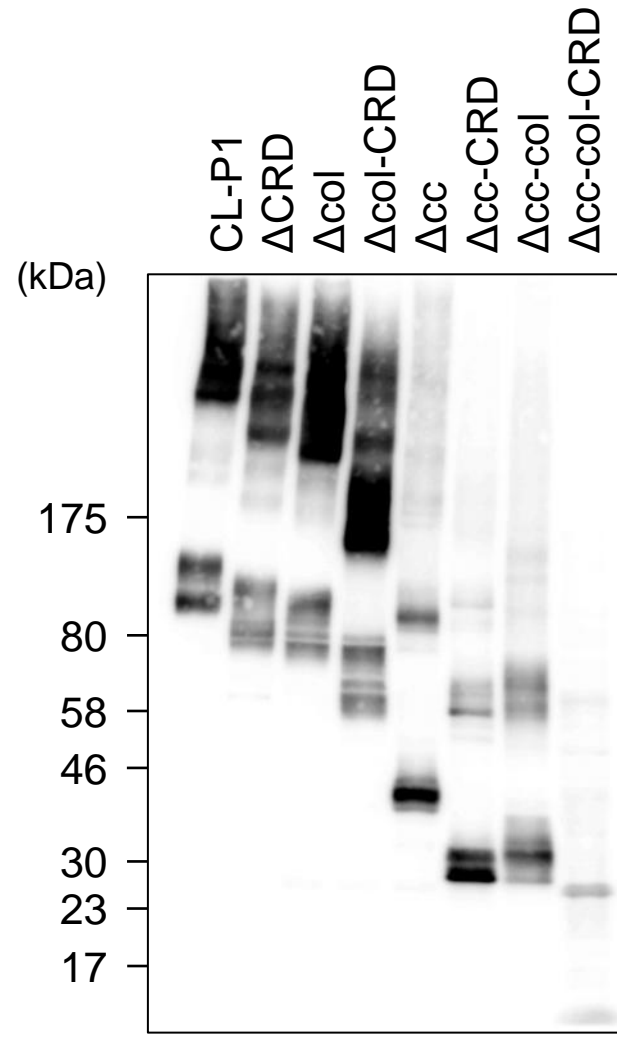


Fig 3

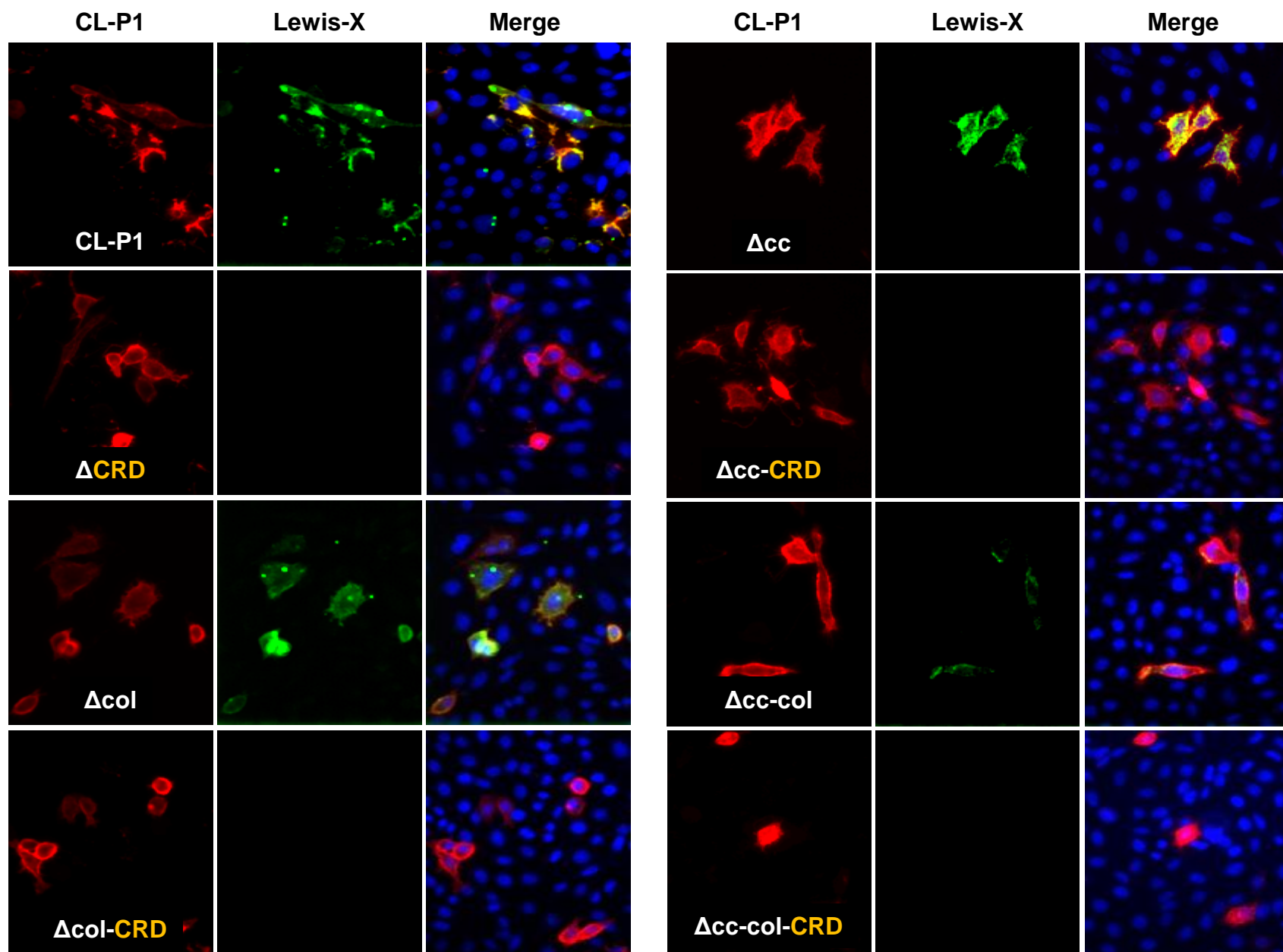


Fig 4 (a)

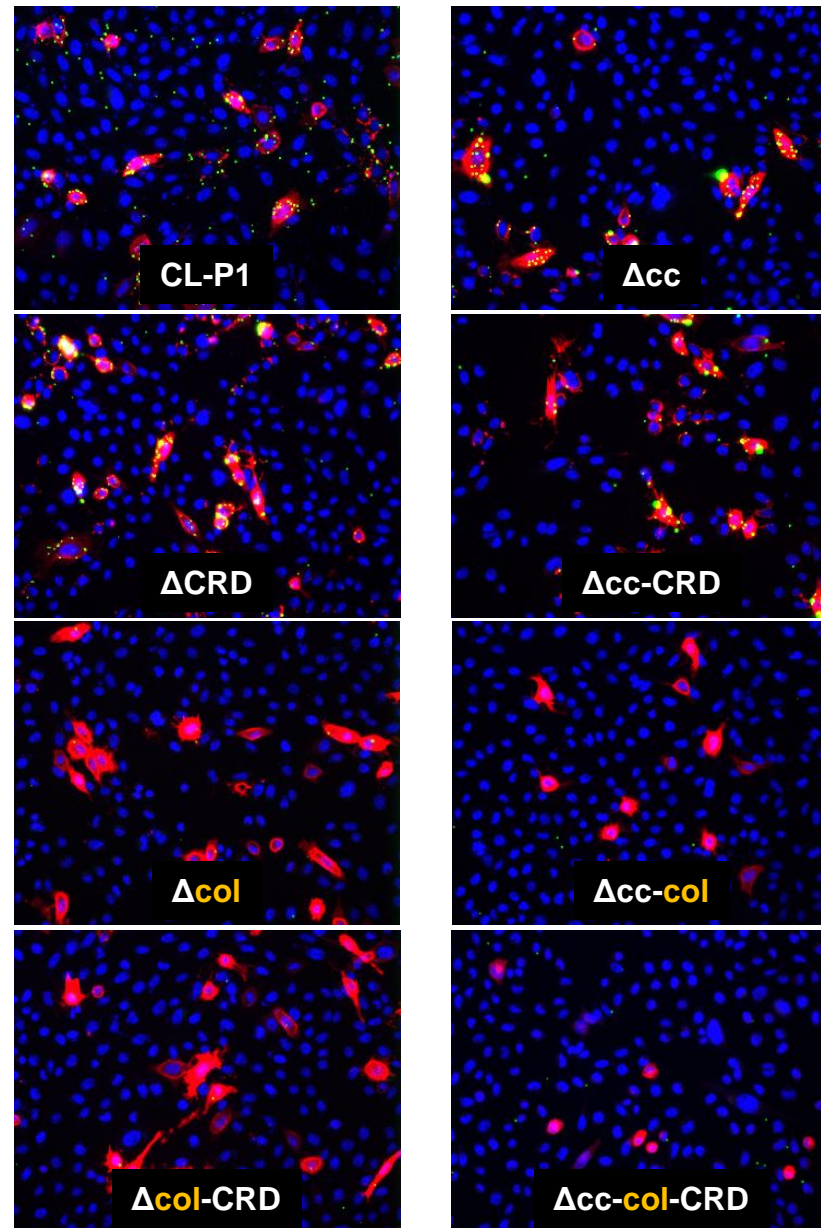


Fig 4 (b)

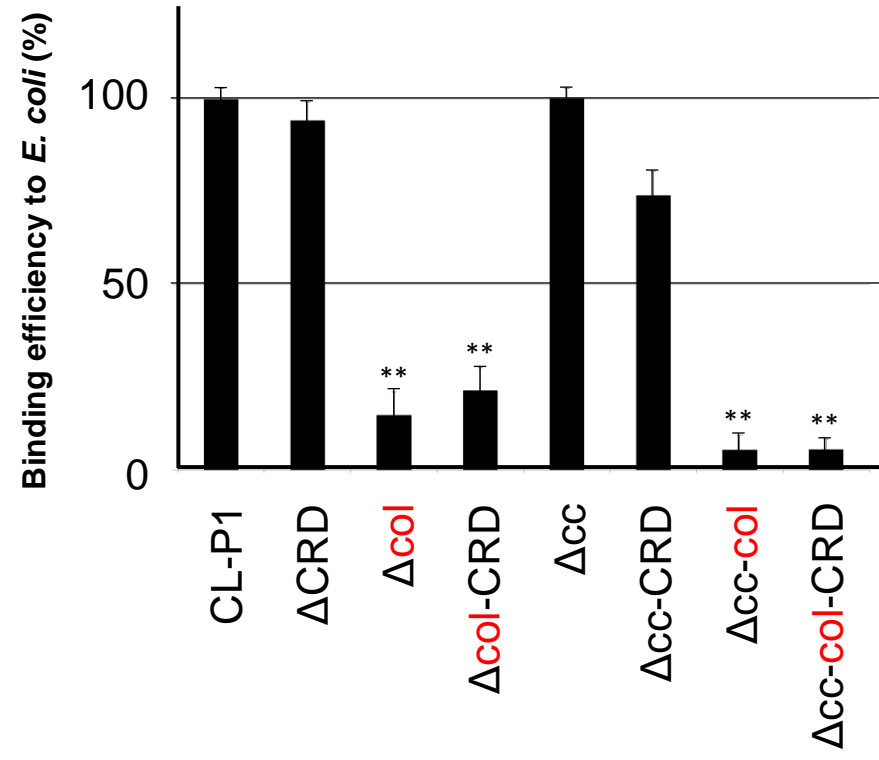


Fig 4 (c)

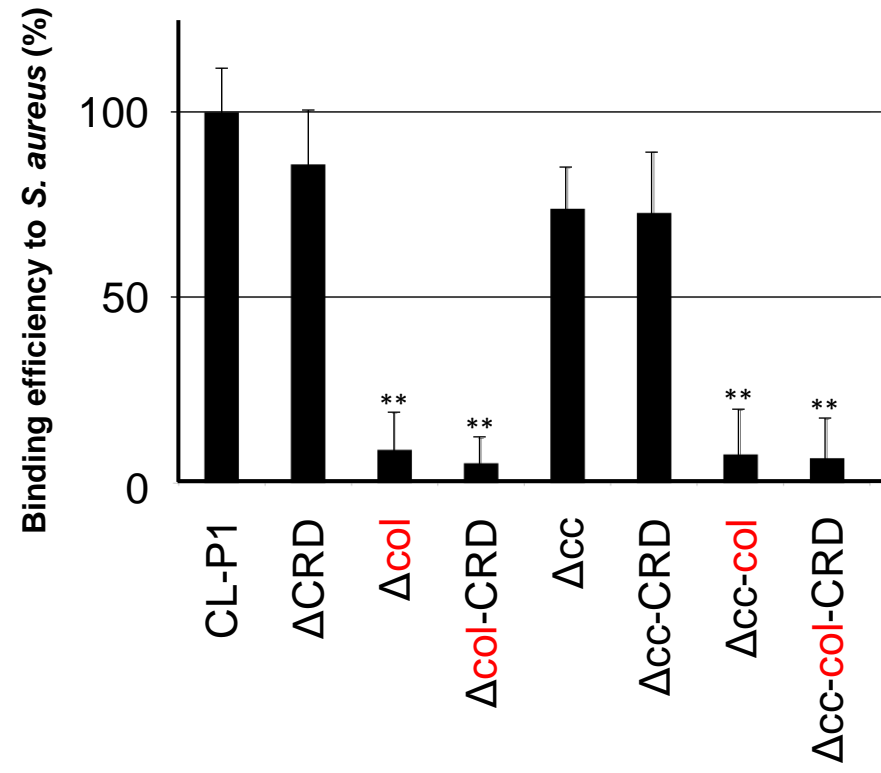


Fig 4 (d)

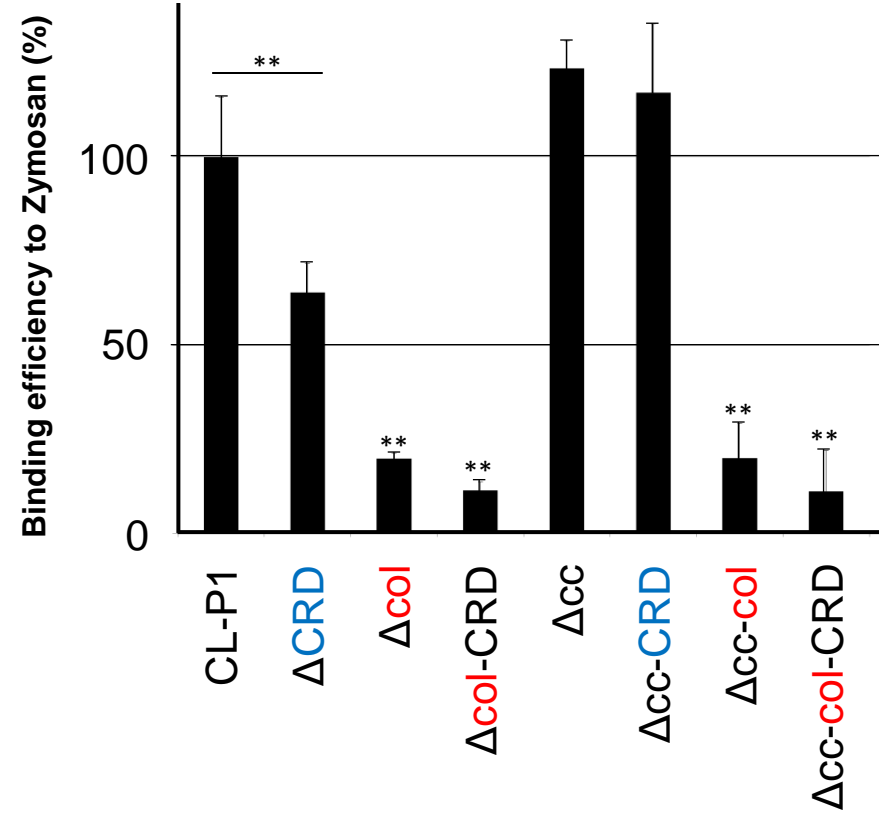


Fig 5 (a)

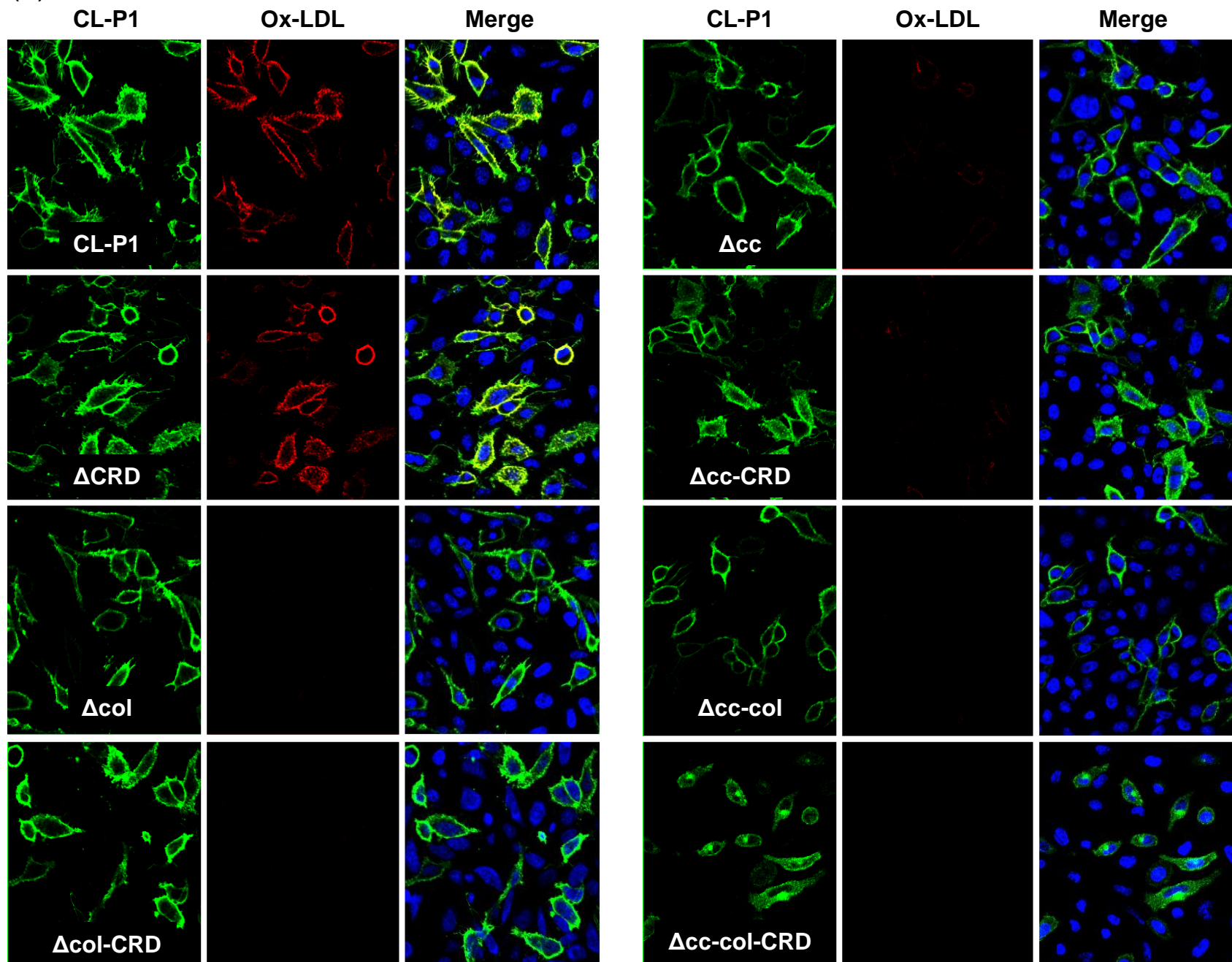


Fig 5 (b)

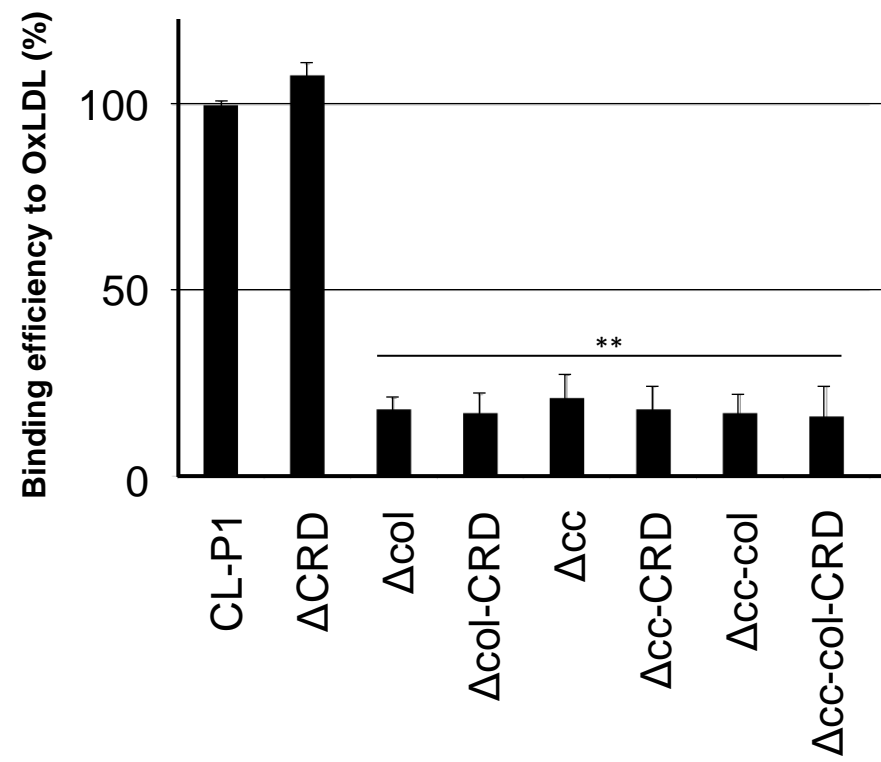


Fig 6 (a)

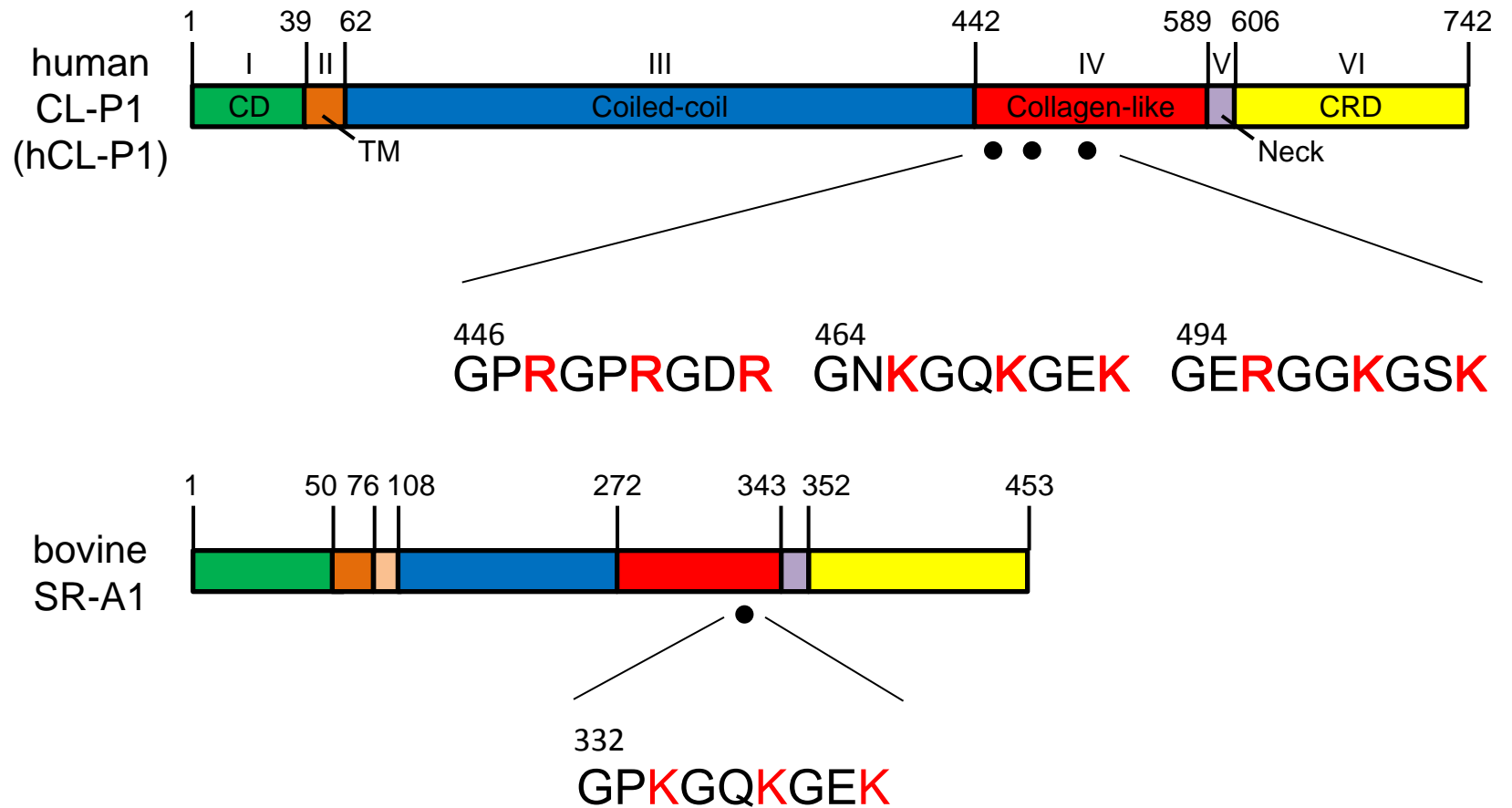
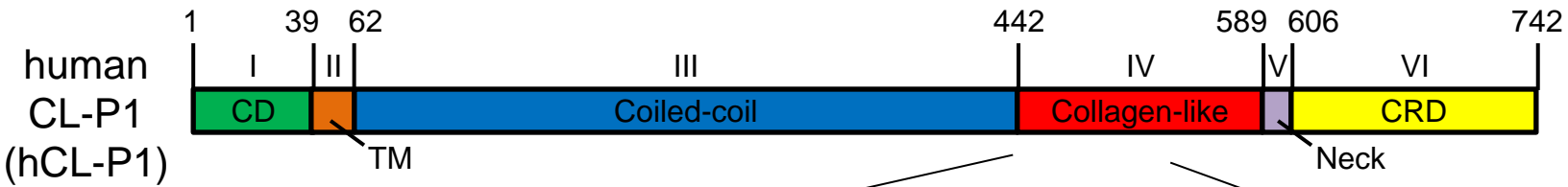


Fig 6 (b)



	446	464	494
hCL-P1	GPR RG PRGDR	GN K GQ K G E K	GER RG G K GSK
M W W	GPR RG PA G DR	GN K GQ K G E K	GER RG G K GSK
W M W	GPR RG PRGDR	GN K GQ A G E K	GER RG G K GSK
W W M	GPR RG PRGDR	GN K GQ K G E K	GER RG G A GSK
M M M	GPR RG PA G DR	GN K GQ A G E K	GER RG G A GSK

Fig 6 (c)

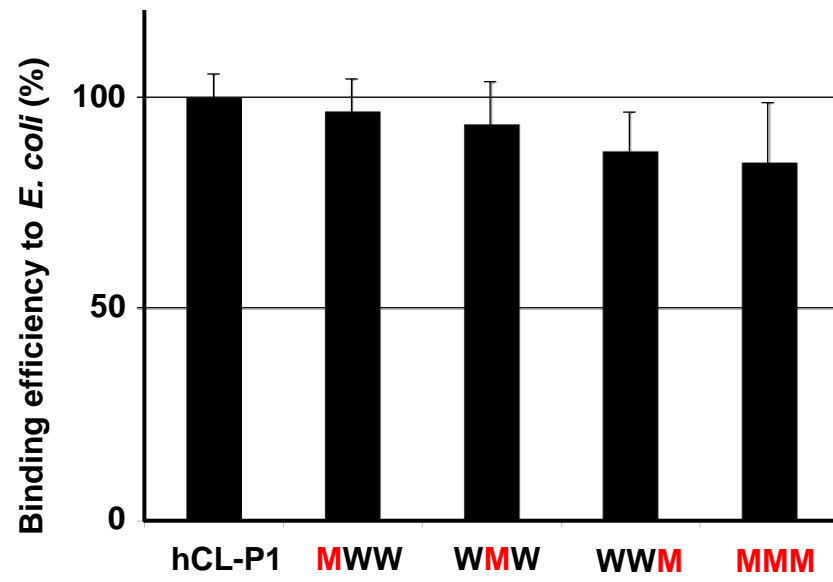


Fig 6 (d)

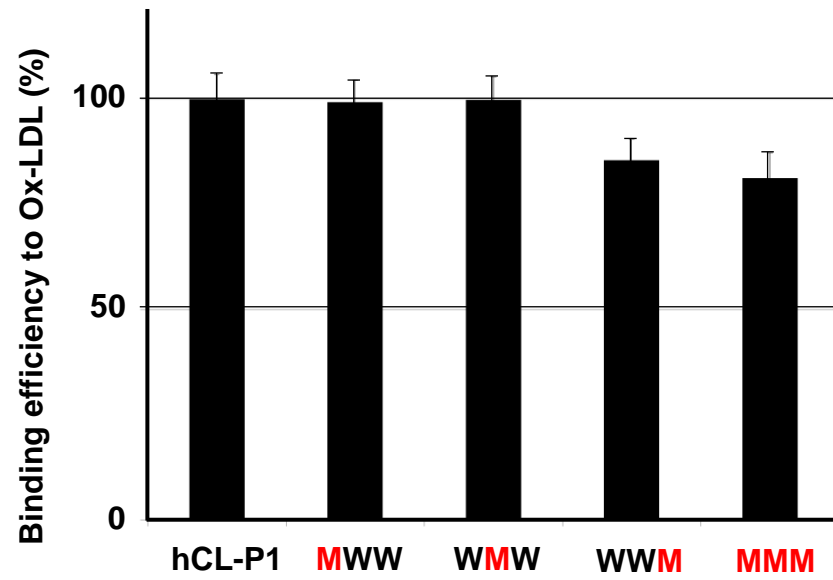
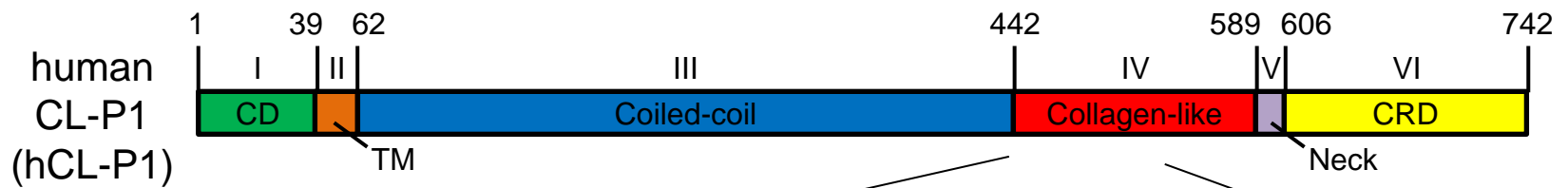


Fig 7 (a)



hCL-P1	446 GPR RGPRGDR	464 GN KGQKGEK	494 GER GGKGSK
Col mutant I	GP AGPAGDA	GN KGQKGEK	GER GGKGSK
Col mutant II	GPR RGPRGDR	GN AGQAGEA	GER GGKGSK
Col mutant III	GPR RGPRGDR	GN KGQKGEK	GE AGGAGSA
Col mutant IV	GP AGPAGDA	GN AGQAGEA	GE AGGAGSA

Fig 7 (b)-I

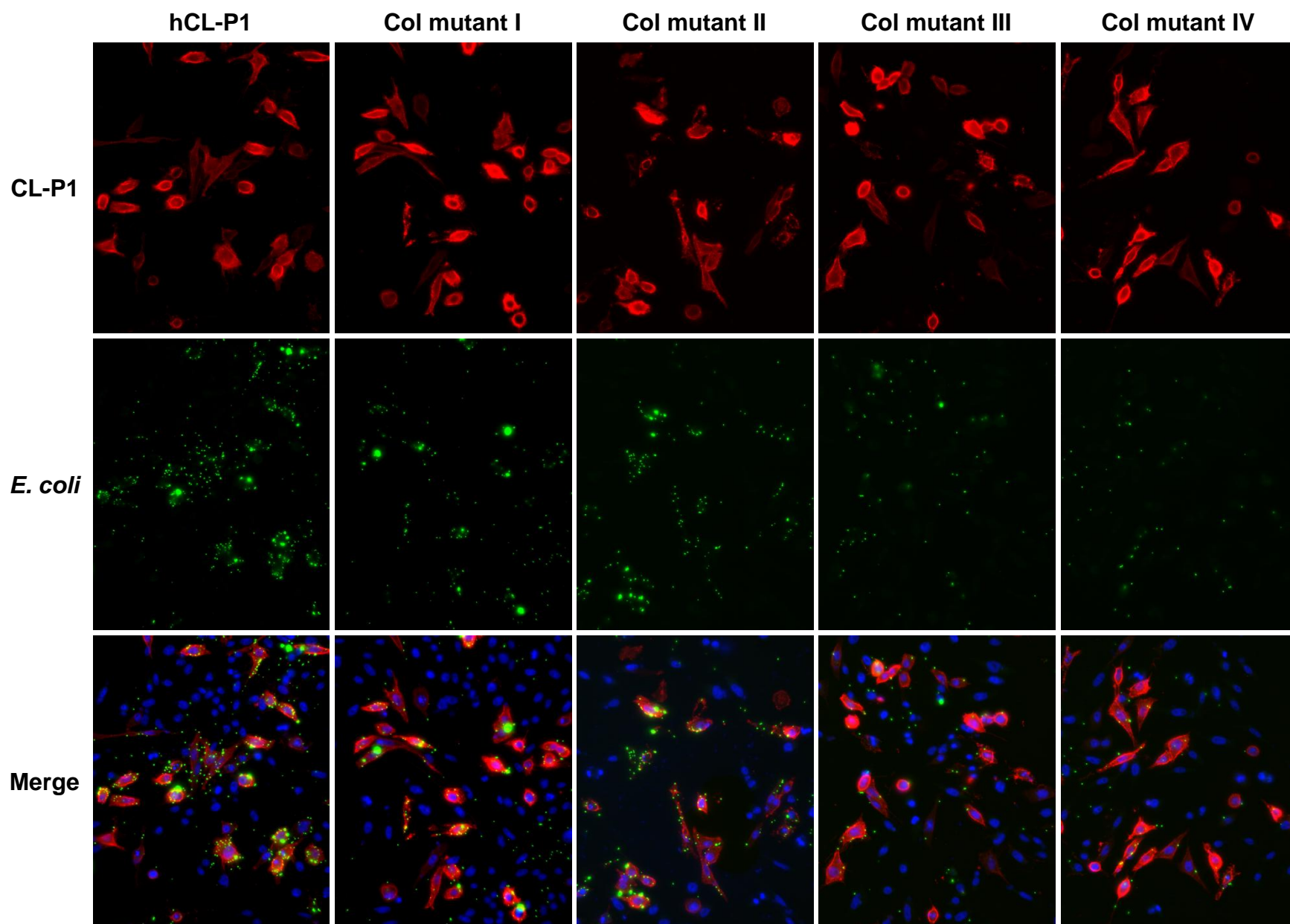


Fig 7 (b)-II

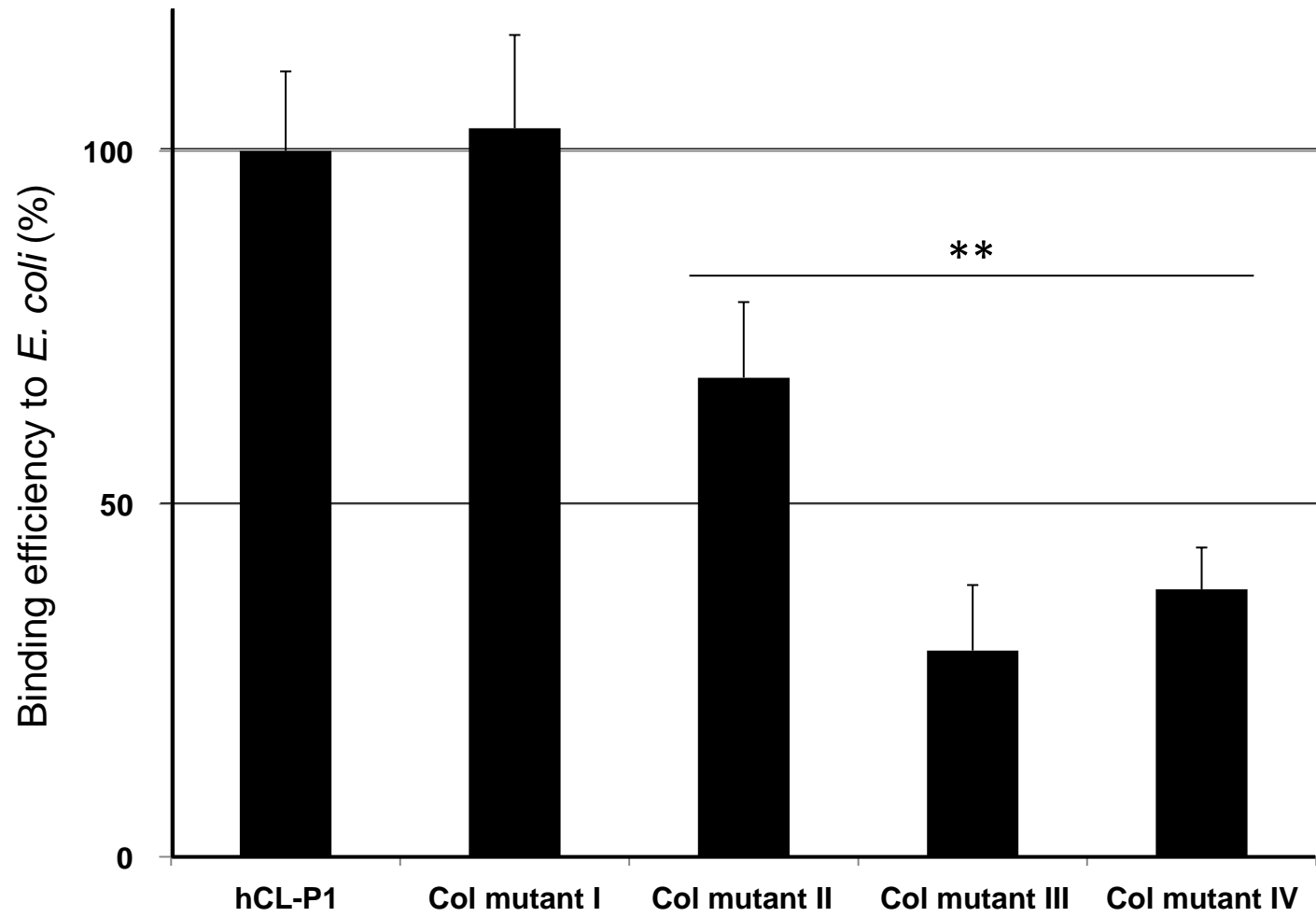


Fig 7 (c)-I

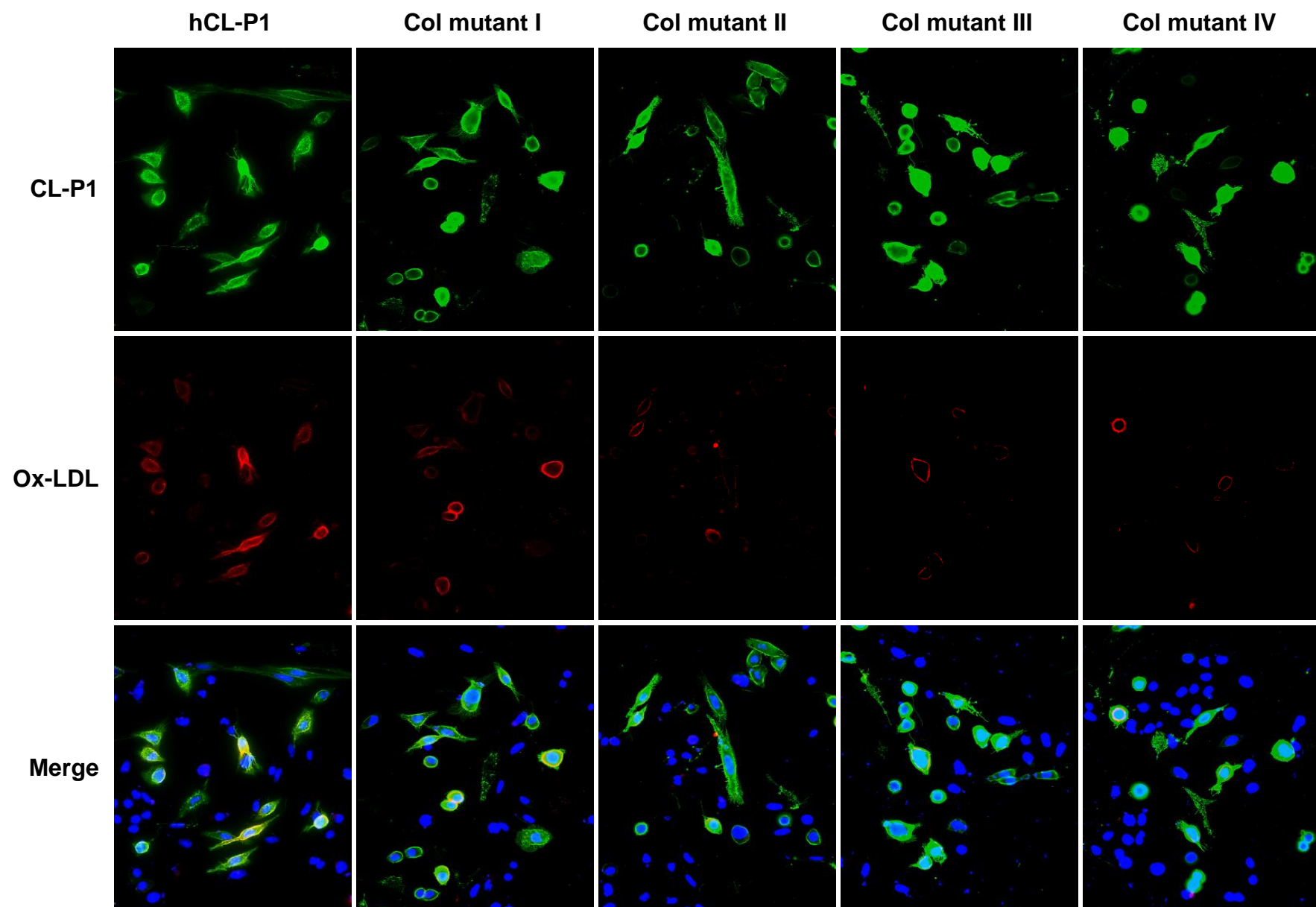


Fig 7 (c)-II

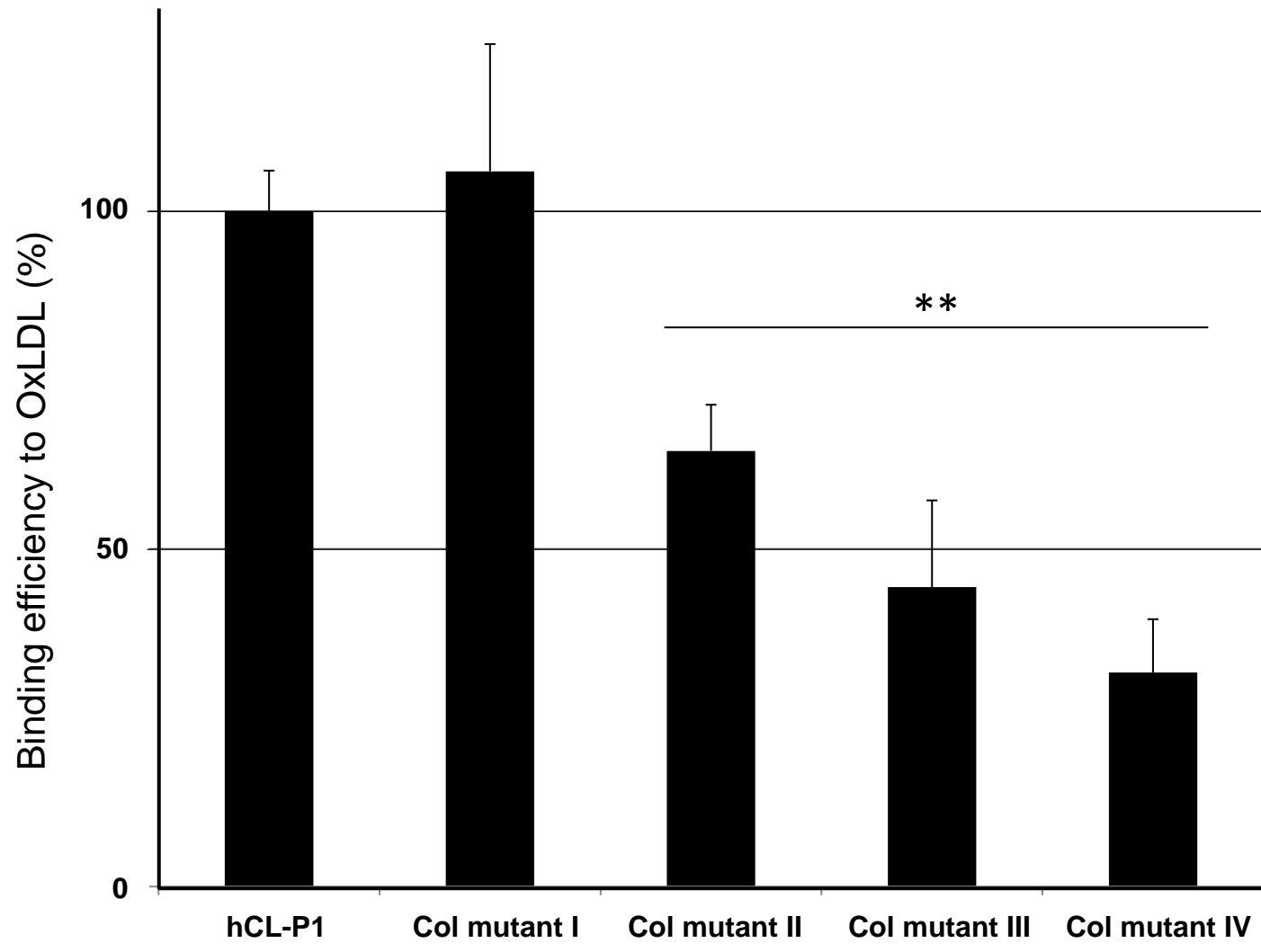
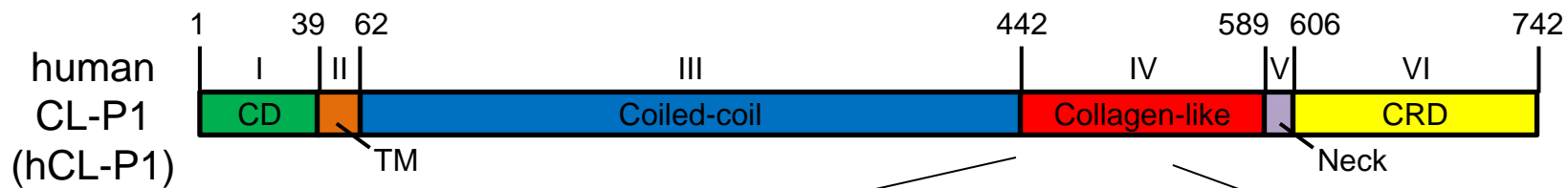


Fig 8



	446	464	494
human	GP RGPRGDR	GN KGQKGEK	GE RGGKGSK
bovine	GP RGPKGDR	GN KGQKGEK	GE RGSKGSK
mouse	GP RGPKGDR	GN KGQKGEK	GE RGSKGSK
rat	GP RGPKGDR	GN KGQKGEK	GE RGSKGSK
chicken	GP RGPKGDR	GL KGQKGEK	GE KGGKGSR
frog	GP RGPKGER	GP KGQMGEK	GE KGSKGSR
zebrafish	GP RGPRGDK	GP KGEKGEK	GL KGPPGSR

Supplementary Material (for online publication)[Click here to download Supplementary Material \(for online publication\): Supplemental Figure 1-4.pptx](#)

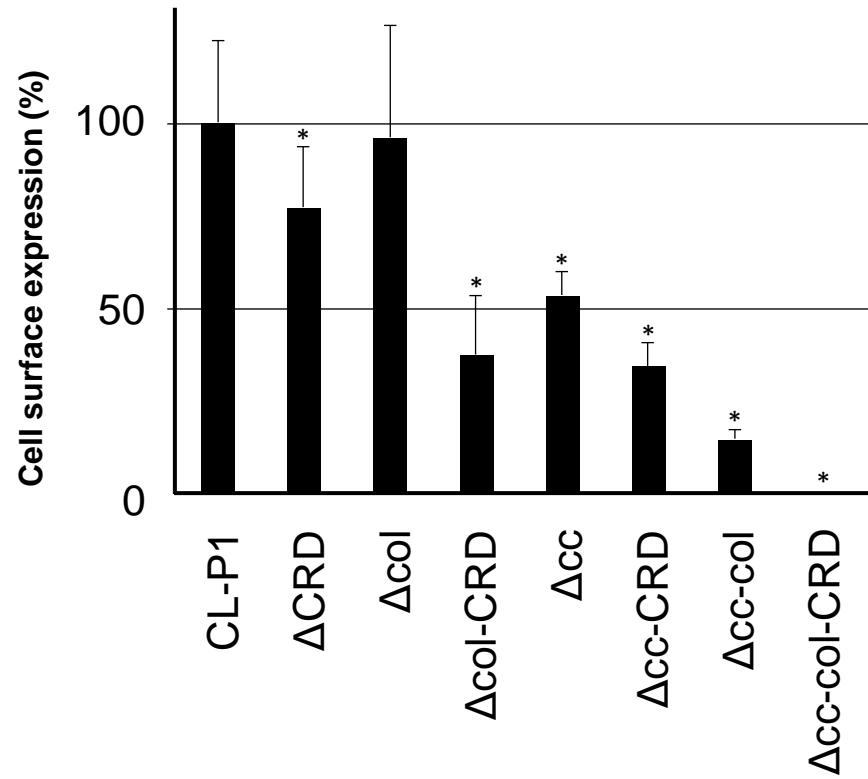
(a) primers	5' to 3'
ON7068 NotI for CRD Fw	TTGCGGCCGCGAGGATGAAAGACGACTTCGCAGA
ON7069 XbaI for CRD Rv	GGTCTAGATAATGCAGATGACAGTACTG
ON7070 XbaI for Neck Rv	CCTCTAGAGCCATTGTCCTCCGGTGCCG
ON7088 AccI for cc-CRDFw, del-col	TAGTAGACTCCAAGCATGGTCAGCTCATCAAGAATTTTACAATACTACAAGTGCCCCCTGGCCCTGCAGAA
ON7060 XbaI for cc Rv	CCTCTAGATTGTAGTATTGTAAAATTCTTGATGAG
ON7085 SgrAI for TM Rv	CCCACCGGTGACATTGTCCATTTTCTC
ON7086 SgrAI for col Fw	CCCACCGGTGGTCCACCGGGCCCCAGGGG
ON7087 SgrAI for CRD Fw	CCCACCGGTGGCCCATCAGGAGCGGTGGT
ON7061 XbaI for TM Rv	CCTCTAGAACCGGTGACATTGTCCATTTTCTC

(b) primers	5' to 3'
ON9056 hCLP1-R496A-F	GGTCCCCCGGAGAGGCTGGCGGCGCAGGATC
ON9057 hCLP1-R496A-R	GATCCTGCGCCGCCAGCCTCTCCGGGGGGACC
ON3009 hCLP1-K499A-F	GGAGAGCGTGGCGGCGCAGGATCTAAAGGC
ON3010 hCLP1-K499A-R	GCCTTTAGATCCTGCGCCGCCACGCTCTCC
ON9058 hCLP1-K502A-F	GGCGGCGCAGGATCTGCAGGCTCCCAGGGCCC
ON9059 hCLP1-K502A-R	GGGCCCTGGGAGCCTGCAGATCCTGCGCCGCC
ON0006 hP1-1RRR-AAA-F	CTAGTAGACTCCAAGCATGGTCAGCTCATCAAGAATTTTACAATACTACAAGGTCCACCGG
ON0007 hP1-1RRR-AAA-R	GTCCCTGGGATCCTGCGTACCTGCTGGACCCGCGGGGGCCCGGTGGACCTTGTAGTATTG
ON0008 hP1-2KKK-AAA-F	GTGACGCAGGATCCCAGGGACCCCCTGGCCCAACTGGCAACGCGGGACAGGCAGGAGAGGGCGGGGAGCCTG
ON0009 hP1-2KKK-AAA-R	GACCAGCTGGTCCAATTGGGCCTCTCTACCCGCAGGGCCAGGTGGTCCAGGCTCCCCCGCCTCTCCTG
ON3007 hCLP1-R451A-F	CCCAGGGGTCCAGCAGGTGACAGAGGATCC
ON3008 hCLP1-R451A-R	GGATCCTCTGTCACCTGCTGGACCCCTGGG
ON2181 hCLP1-K469A-F	GGCAACAAGGGACAGGCAGGAGAGAAGGGG
ON2182 hCLP1-K469A-R	CCCCTTCTCTCCTGCCTGTCCCTTGTTGCC

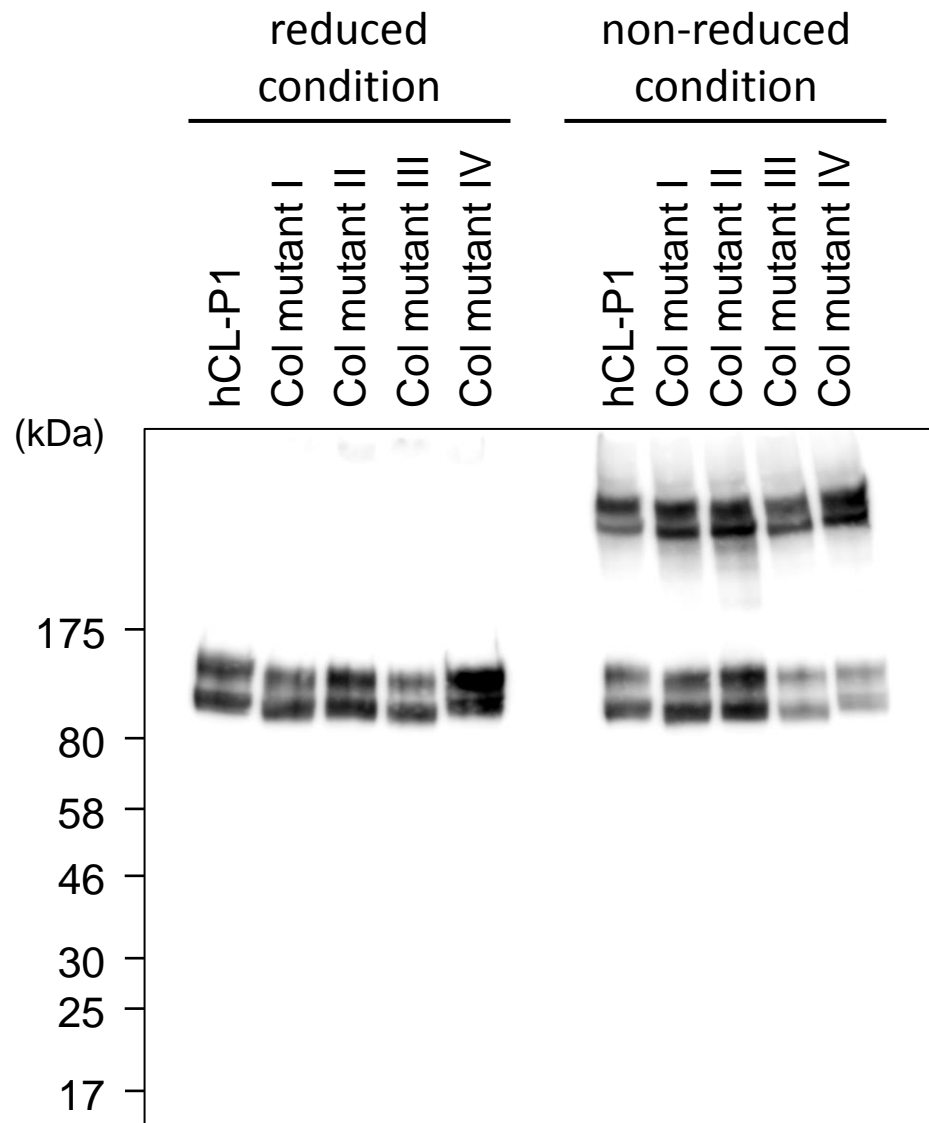
Supplemental Figure 1. List of primers used in this study.

(a) Primers used in CL-P1 deletion mutant construction.

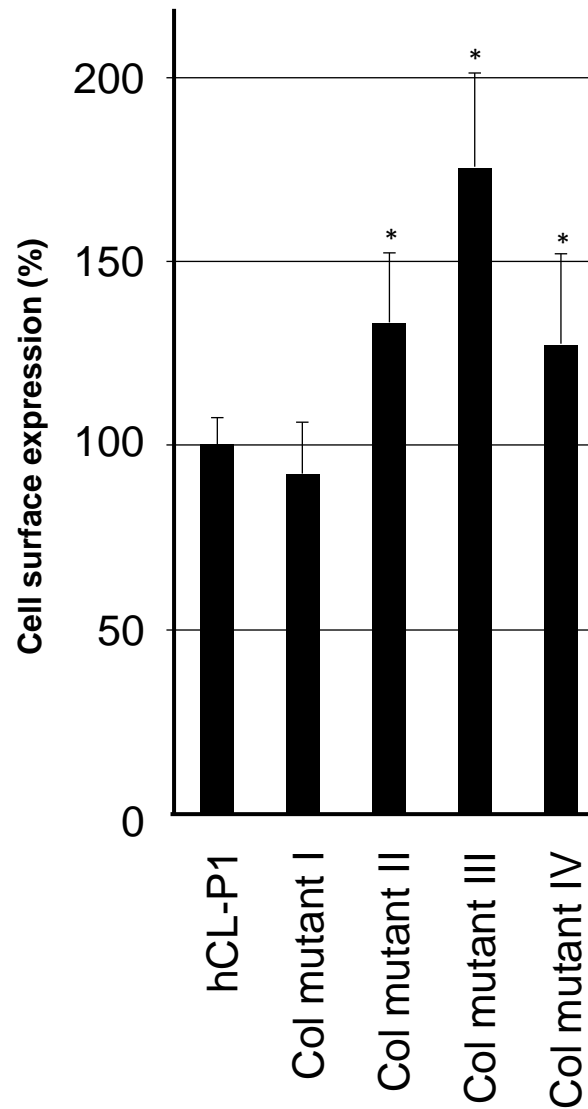
(b) Primers used in CL-P1 collagen-like domain positively charged cluster mutant construction.



Supplemental Figure 2. The cell surface expression level of complete CL-P1 and deletion mutants.



Supplemental Figure 3. Structure patterns in SDS-PAGE and western blotting in CL-P1 and Col mutant I, II, III, and IV.



Supplemental Figure 4. The cell surface expression level of complete CL-P1 and Col mutant I, II, III, and IV.